*Biochimica et Biophysica Acta*, 1059 (1991) 293–311

*ADONIS* 000527289100205O



BBABIO 43459

# A graph-theoretic analysis of metabolic regulation in linear pathways with multiple feedback loops and branched pathways

Asok K. Sen

*Department of Mathematical Sciences, Purdue University School of Science, Indianapolis, IN (U.S.A.)*

(Received 19 December 1990)
(Revised manuscript received 29 April 1991)

Key words: Metabolic regulation; Theoretical model; Graph-theoretic analysis; Flux control coefficient

**With the aid of signal flow graphs, we have analyzed the flux-control distribution in linear metabolic pathways with multiple feedback loops and branched pathways. It is shown that the flux control coefficients of the enzymes in a linear pathway with multiple feedback loops can be evaluated by modifying the signal flow graph of the unregulated pathway in a step-by-step fashion. On the basis of the results obtained with the signal flow graphs, a principle of superposition is suggested for calculating the flux control coefficients of a linear pathway with a general pattern of feedback inhibition. Using this superposition principle, it is possible to determine the flux control coefficients directly from an examination of the topology of the feedback loops in the metabolic pathway, without drawing a signal flow graph. In a branched pathway the control coefficients of the enzymes depend on the fluxes through the various branches in addition to the enzyme elasticities. We show how these fluxes can be incorporated into a signal flow graph from which the flux control coefficients are found. We also describe a systematic procedure for converting a signal flow graph to a simpler form which may significantly reduce the effort necessary for calculating the flux control coefficients. Modifications of a signal flow graph for assessing the relative importance of the enzymes in flux control are also discussed. Based on our findings from the signal flow graphs, we have presented a heuristic method for determining the flux control coefficients directly from the reaction sequence of the pathway, without drawing a signal flow graph. The present analysis applies to metabolic pathways in a steady state.**

## Introduction

Graph theory is found to be a valuable tool in a variety of physical applications. It often provides a visual framework for a quantitative analysis of the behavior of the system under consideration. A graph-theoretic technique which has been widely used in the analysis of electric and electronic circuits is known as the method of signal flow graphs [1–3]. We have recently demonstrated [4] that a signal flow graph can be utilized for control analysis of metabolic pathways in the steady state. In [4], we analyzed the control properties of (i) a linear pathway with no feedback or feedforward regulation; this will be referred to here as the *unregulated* pathway; (ii) a linear pathway in which the first enzyme undergoes feedback inhibition by the last variable metabolite. For the unregulated pathway, the control structure is represented by a signal flow graph. The flux control coefficients of the various enzymes are evaluated directly from the signal flow graph, without the use of algebraic procedures such as matrix inversion. The signal flow graph of the unregulated pathway is subsequently modified to account for feedback inhibition, in pathway (ii).

The objective of the present work is to show that the flux control coefficients of a linear pathway with multiple feedback loops can be calculated by modifying the signal flow graph of the unregulated pathway in a step-by-step fashion. On the basis of the results obtained with the signal flow graphs, a principle of superposition is suggested for calculating the flux control coefficients of a linear pathway with a general pattern of feedback inhibition. Using this superposition principle, it is possible to determine the flux control coefficients directly from an examination of the topology of the feedback loops in the pathway, without drawing a signal flow graph. In a linear pathway the control

Correspondence: A.K. Sen, Department of Mathematical Sciences, Purdue University School of Science, 1125 East 38th Street, Indianapolis, IN. 46205, U.S.A.

coefficients of the enzymes depend only on their elasticity coefficients. The control coefficients of a branched pathway, on the other hand, depend also on the fluxes through the different branches. We will show how these fluxes can be incorporated into a signal flow graph from which the flux control coefficients are evaluated. We will also describe a systematic procedure for simplifying the structure of a signal flow graph which may significantly reduce the effort necessary for calculating the flux control coefficients. Modifications of a signal flow graph for determining the relative proportions of flux control of the various enzymes are also discussed. Based on our findings from the signal flow graphs, we have presented a heuristic method for determining the flux control coefficients directly from the reaction sequence of the pathway, without drawing a signal flow graph. As in [4], the present analysis is based on Metabolic Control Theory which was formulated by Kacser and Burns [5] and Heinrich and Rapoport [6].

Within the premises of Metabolic Control Theory, several alternate approaches have been developed earlier for evaluating the control coefficients of metabolic pathways. These include matrix inversion techniques [7–9], diagrammatic methods [10], electrical analogs [11,12], graphical procedures [13,14] and a structural approach [15].

**Review of previous work**

To set the stage for the present work, we consider a simple linear pathway with no feedback or feedforward regulation (Scheme A). This pathway was analyzed in an earlier paper [4] using signal flow graphs. Here the six enzymes are designated by the letter E with appropriate subscripts; the initial substrate $X_1$ and the final product P are fixed metabolites (i.e., they are kept at fixed concentration levels), whereas $X_2$ through $X_6$ represent variable metabolites. A signal flow graph for deriving the flux control coefficients of the enzymes in this pathway is shown in Fig. 1. This figure is reproduced from [4]; note, however, a slight change of notation. In this figure the nodes 1–6 represent the unknown flux control coefficients of the enzymes $E_1$–$E_6$; node 7 is the source node. The symbol $\varepsilon_j^i$ denotes the elasticity coefficient of an enzyme $E_i$ with respect to the metabolite $X_j$. In particular, if $\varepsilon_j^i$ is an elasticity coefficient due to product inhibition, then it is written as $\varepsilon_j^i = -\bar{\varepsilon}_j^i$, $\bar{\varepsilon}_j^i$ being the absolute magnitude of $\varepsilon_j^i$. The weight on the directed edge from node $i$ to node $i+1$ ($i = 1, 2, 3, 4, 5$) is equal to the ratio of the absolute magnitudes of the elasticity coefficients of the contiguous pair of enzymes $E_i$ and $E_{i+1}$ with respect to their linking metabolite $X_{i+1}$.

$$X_1 \xrightarrow{E_1} X_2 \xrightarrow{E_2} X_3 \xrightarrow{E_3} X_4 \xrightarrow{E_4} X_5 \xrightarrow{E_5} X_6 \xrightarrow{E_6} P$$

Scheme A

From the signal flow graph, the flux control coefficient of an enzyme $E_i$ can be found with the aid of the formula

$$C_i^J = \frac{1}{\Delta}\sum_k G_{ki}\Delta_{ki}, \tag{1}$$

where

$$\Delta = 1 - L_1 + L_2 - L_3 + \ldots, \tag{2}$$

$L_1$, $L_2$,... being the sum of the gains of all first-order cycles, second-order cycles, etc. in Fig. 1. The quantity $G_{ki}$ denotes the gain of the $k$-th directed path from the source node to node $i$, and $\Delta_{ki}$ is the part of $\Delta$ (including the first term of 1) which corresponds to those cycles that do not touch the $k$-th directed path from the source node to node $i$. A directed path from a node $i$ to a node $j$ is a sequence of directed edges which starts at node $i$ and ends at node $j$. A directed path whose beginning and ending nodes are the same forms a cycle. The gain of a directed path or a cycle is the product of the weights on all its edges. The reader is referred to Ref. 4 for other graph-theoretic definitions used above.

The signal flow graph of Fig. 1 has five first-order cycles, and no second- or higher order cycles. The first-order cycles are formed by the edges (i) (1,2) and (2,1), (ii) (1,2), (2,3) and (3,1), (iii) (1,2), (2,3), (3,4) and (4,1), (iv) (1,2) (2,3), (3,4), (4,5) and (5,1), and (v) (1,2), (2,3), (3,4), (4,5), (5,6) and (6,1). With the gains of these first-order cycles we find from Eqn. 2:

$$\Delta^0 = 1 + \Delta_1 + \Delta_2 + \Delta_3 + \Delta_4 + \Delta_5, \tag{3}$$

where

$$\Delta_1 = \frac{\bar{\varepsilon}_2^1}{\varepsilon_2^2}, \Delta_2 = \frac{\bar{\varepsilon}_2^1\bar{\varepsilon}_3^2}{\varepsilon_2^2\varepsilon_3^3}, \Delta_3 = \frac{\bar{\varepsilon}_2^1\bar{\varepsilon}_3^2\bar{\varepsilon}_4^3}{\varepsilon_2^2\varepsilon_3^3\varepsilon_4^4}, \Delta_4 = \frac{\bar{\varepsilon}_2^1\bar{\varepsilon}_3^2\bar{\varepsilon}_4^3\bar{\varepsilon}_5^4}{\varepsilon_2^2\varepsilon_3^3\varepsilon_4^4\varepsilon_5^5},$$

$$\Delta_5 = \frac{\bar{\varepsilon}_2^1\bar{\varepsilon}_3^2\bar{\varepsilon}_4^3\bar{\varepsilon}_5^4\bar{\varepsilon}_6^5}{\varepsilon_2^2\varepsilon_3^3\varepsilon_4^4\varepsilon_5^5\varepsilon_6^6}. \tag{4}$$

The zero superscript on $\Delta$ indicates that it applies to the unregulated pathway. Note that there is only one directed path from the source node to each of the nodes 1 through 6 in Fig. 1, and all the cycles touch each of these directed paths. Using the gains of these directed paths in Eqn. 1 we obtain

$$C_1^J = 1/\Delta^0, C_2^J = \Delta_1/\Delta^0, C_3^J = \Delta_2/\Delta^0, C_4^J = \Delta_3/\Delta^0, C_5^J = \Delta_4/\Delta^0,$$

$$C_6^J = \Delta_5\Delta^0 \tag{5}$$

with $\Delta^0$ given by Eqn. 3. For future reference, note that the term $\Delta_1$ is equal to the ratio of the magnitudes

of the elasticity coefficients of the first two enzymes in the pathway, with respect to their shared metabolite; the term $\Delta_2$ is the product of $\Delta_1$ and the ratio of the magnitudes of the elasticity coefficients of the enzymes $E_2$ and $E_3$ towards the metabolite $X_3$; the term $\Delta_3$ is equal to $\Delta_2$ times $\bar{\varepsilon}_4^3/\varepsilon_4^4$, and so on.

**Topology of multiple feedback loops**

As mentioned in the Introduction, the flux control coefficients of a linear pathway with multiple feedback loops can be determined by modifying the signal flow graph of the unregulated pathway in a step-by-step fashion. To illustrate this procedure, we first investigate the topology of two overlapping feedback loops, i.e., those which have at least one enzyme or one metabolite in common. In particular we consider the scenario in which the two feedback loops lie completely one inside the other as shown in Scheme B. A signal flow graph for this pathway is shown in Fig. 2, which is generated from Fig. 1 by incorporating the effects of the feedback loops in the following manner. Consider the outer feedback loop first. To include the effect of this feedback loop, we delete all the enzymes and metabolites in the pathway that lie inside the feedback loop and treat the enzymes $E_1$ and $E_6$ as contiguous enzymes with $X_6$ as their adjoining metabolite. Accordingly, in Fig. 1 we introduce a directed edge from node 1 to node 6 with a weight equal to $\bar{\varepsilon}_6^1/\varepsilon_6^6$, $\bar{\varepsilon}_6^1$ being the absolute magnitude of the elasticity coefficient of enzyme $E_1$ due to feedback inhibition (see also Ref. 4). Similarly, corresponding to the inner feedback loop, a directed edge is inserted in Fig. 1 from node 3 to node 5. This directed edge carries a weight equal to $\bar{\varepsilon}_5^3/\varepsilon_5^5$, where $\bar{\varepsilon}_5^3$ is the absolute value of the elasticity coefficient of enzyme $E_3$ due to feedback inhibition. It is evident that Fig. 2 has three first-order cycles in addition to those present in Fig. 1, and there are no second- or higher order cycles. The three cycles consist of (i) the edge (1,6) and (6,1) joining the nodes 1 and 6, (ii) the edges (1,2), (2,3), (3,5) and (5,1) connecting the nodes 1, 2, 3 and 5, and (iii) the edges (1,2), (2,3), (3,5), (5,6) and (6,1) passing through the nodes 1, 2, 3, 5 and 6. These cycles contribute three additional terms in the denominator $\Delta$ of Eqn. 1, which is now expressed as

$$\hat{\Delta} = \Delta^0 + \frac{\bar{\varepsilon}_6^1}{\varepsilon_6^6} + \frac{\bar{\varepsilon}_2^1\bar{\varepsilon}_3^2\bar{\varepsilon}_5^3}{\varepsilon_2^2\varepsilon_3^3\varepsilon_5^5} + \frac{\bar{\varepsilon}_2^1\bar{\varepsilon}_3^2\bar{\varepsilon}_5^3\bar{\varepsilon}_6^5}{\varepsilon_2^2\varepsilon_3^3\varepsilon_5^5\varepsilon_6^6}. \tag{6}$$

It is easily seen that the directed paths from the source node to the nodes 1, 2, 3 and 4 in Fig. 2 are identical to those in Fig. 1, and all the cycles in Fig. 2 touch each of these directed paths. Thus $C_1^J = 1/\hat{\Delta}$, $C_2^J = \Delta_1/\hat{\Delta}$, $C_3^J = \Delta_2/\hat{\Delta}$, and $C_4^J = \Delta_3/\hat{\Delta}$. There are, however, two directed paths from the source node to node 5 in Fig. 2; the gains of these directed paths lead to

$$C_5^J = \frac{1}{\hat{\Delta}}\left[\Delta_4 + \frac{\bar{\varepsilon}_2^1\bar{\varepsilon}_3^2\bar{\varepsilon}_5^3}{\varepsilon_2^2\varepsilon_3^3\varepsilon_5^5}\right]. \tag{7}$$

Finally the flux control coefficient of enzyme $E_6$ is found by examining the three directed paths from the source node to node 6 in Fig. 2. It follows that

$$C_6^J = \frac{1}{\hat{\Delta}}\left[\Delta_5 + \frac{\bar{\varepsilon}_6^1}{\varepsilon_6^6} + \frac{\bar{\varepsilon}_2^1\bar{\varepsilon}_3^2\bar{\varepsilon}_5^3\bar{\varepsilon}_6^5}{\varepsilon_2^2\varepsilon_3^3\varepsilon_5^5\varepsilon_6^6}\right]. \tag{8}$$

The quantities $\Delta_1$ through $\Delta_5$ are given in Eqn. 4.

We would like to point out that the expressions for the flux control coefficients of this pathway do not contain any term involving the product $\bar{\varepsilon}_6^1\bar{\varepsilon}_5^3$, of the elasticity coefficients of the two feedback loops. This is due to the fact that two feedback loops in the pathway overlap each other., We shall see later that if a pathway contains two non-overlapping feedback loops, then some of the control coefficients may depend on the product of the elasticity coefficients of the non-overlapping feedback loops.

There are a few other configurations in which two feedback loops can exist in an overlapping fashion. These include a pathway where (i) the same enzyme is inhibited by two different metabolites, (ii) the same metabolite inhibits two different enzymes, and (iii) two enzymes are inhibited by two different metabolites in an overhanging pattern as shown in Scheme C.

We now examine a pathway containing two non-overlapping feedback loops, i.e., the two loops have no enzyme or no metabolites in common between them (Scheme D). Fig. 3 depicts a signal flow graph for the control structure of this pathway. This figure is drawn from Fig. 1 with the addition of two edges, one directed from node 1 to node 3 and the other directed from node 4 to node 6, corresponding to the left and the right feedback loops, respectively. The weights on these edges are as shown. The symbols $\bar{\varepsilon}_3^1$ and $\bar{\varepsilon}_6^4$

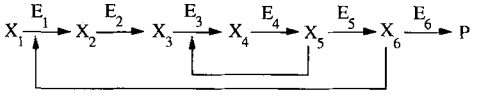


Scheme B

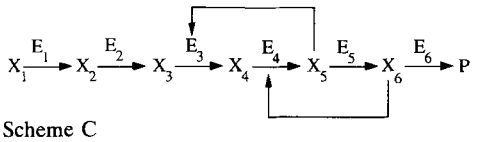


Scheme C

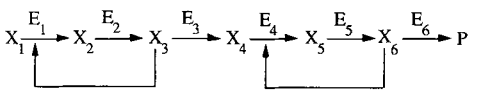


Scheme D

indicate the absolute magnitudes of the elasticity coefficients of the enzymes $E_1$ and $E_4$ due to feedback inhibition by the metabolites $X_3$ and $X_6$, respectively. It is easy to see that there are six first order cycles in this figure in addition to those present in Fig. 1; there are no second- or higher order cycles. Substituting the gains of these cycles into Eqn. 2, we find

$$\bar{\Delta} = \Delta^0 + \frac{\bar{\varepsilon}_3^1}{\varepsilon_3^3} + \frac{\bar{\varepsilon}_3^1\bar{\varepsilon}_4^3}{\varepsilon_3^3\varepsilon_4^4} + \frac{\bar{\varepsilon}_3^1\bar{\varepsilon}_4^3\bar{\varepsilon}_5^4}{\varepsilon_3^3\varepsilon_4^4\varepsilon_5^5} + \frac{\bar{\varepsilon}_3^1\bar{\varepsilon}_4^3\bar{\varepsilon}_5^4\bar{\varepsilon}_6^5}{\varepsilon_3^3\varepsilon_4^4\varepsilon_5^5\varepsilon_6^6} + \frac{\bar{\varepsilon}_2^1\bar{\varepsilon}_3^2\bar{\varepsilon}_4^3\bar{\varepsilon}_6^4}{\varepsilon_2^2\varepsilon_3^3\varepsilon_4^4\varepsilon_6^6} + \frac{\bar{\varepsilon}_3^1\bar{\varepsilon}_4^3\bar{\varepsilon}_6^4}{\varepsilon_3^3\varepsilon_4^4\varepsilon_6^6}. \tag{9}$$

The overbar on $\Delta$ implies that is applies to pathway D. Note that in contrast to the results obtained earlier, the expression for $\bar{\Delta}$ contains a term (viz., the last term) involving the product of the elasticity coefficients, $\bar{\varepsilon}_3^1$ and $\bar{\varepsilon}_6^4$, of both feedback-inhibited enzymes. This term results from the cycle connecting the nodes 1, 3, 4 and 6 in Fig. 3, and is a characteristic of a non-overlapping pattern of feedback loops. From an inspection of the directed path from the source node to the nodes 1 and 2, the flux control coefficients of the first two enzymes in this pathway are found to be: $C_1^J = 1/\bar{\Delta}$ and $C_2^J = \Delta_1/\bar{\Delta}$. Examination of the two directed paths from the source node to nodes 3, 4 and 5, respectively, reveals that

$$C_3^J = \frac{1}{\bar{\Delta}}\left[\Delta_2 + \frac{\bar{\varepsilon}_3^1}{\varepsilon_3^3}\right], C_4^J = \frac{1}{\bar{\Delta}}\left[\Delta_3 + \frac{\bar{\varepsilon}_3^1\bar{\varepsilon}_4^3}{\varepsilon_3^3\varepsilon_4^4}\right], C_5^J = \frac{1}{\bar{\Delta}}\left[\Delta_4 + \frac{\bar{\varepsilon}_3^1\bar{\varepsilon}_4^3\bar{\varepsilon}_5^4}{\varepsilon_3^3\varepsilon_4^4\varepsilon_5^5}\right]. \tag{10}$$

To find $C_6^J$, notice that there are three directed paths from the source node to node 6 in Fig. 3. From the gains of these directed paths, we obtain

$$C_6^J = \frac{1}{\bar{\Delta}}\left[\Delta_5 + \frac{\bar{\varepsilon}_3^1\bar{\varepsilon}_4^3\bar{\varepsilon}_5^4\bar{\varepsilon}_6^5}{\varepsilon_3^3\varepsilon_4^4\varepsilon_5^5\varepsilon_6^6} + \frac{\bar{\varepsilon}_2^1\bar{\varepsilon}_3^2\bar{\varepsilon}_4^3\bar{\varepsilon}_6^4}{\varepsilon_2^2\varepsilon_3^3\varepsilon_4^4\varepsilon_6^6} + \frac{\bar{\varepsilon}_3^1\bar{\varepsilon}_4^3\bar{\varepsilon}_6^4}{\varepsilon_3^3\varepsilon_4^4\varepsilon_6^6}\right]. \tag{11}$$

*A superposition principle*

On the basis of the results obtained with the signal flow graphs, we suggest below a principle of superposition for calculating the flux control coefficients of a linear metabolic pathway with a general pattern of feedback inhibition. Using this superposition principle, it is possible to determine the flux control coefficients directly from an examination of the topology of the feedback loops in the pathway, without drawing a signal flow graph. As an illustration, we consider the following pathway with both overlapping and non-overlapping feedback loops (Scheme E). The flux control

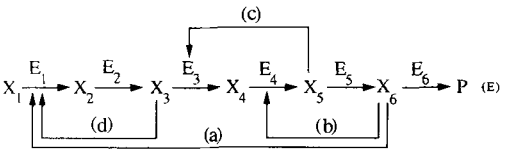


Scheme E

coefficient of an enzyme $E_i$ $(i = 1,2,3,4,5,6)$ in this pathway can be obtained in the form

$$C_i^J = \frac{\text{NUM}}{\text{DEN}}, \tag{12}$$

where NUM and DEN are abbreviations of numerator and denominator, respectively. The denominator DEN can be written as DEN = $\Delta^0$ + additional terms, $\Delta^0$ being the denominator for the unregulated pathway, given by Eqn. 3. Recall that the terms in $\Delta^0$ are formed by taking continued products of the ratios of the magnitudes of the elasticity coefficients of each contiguous pair of enzymes in the unregulated pathway (see the paragraph following Eqn. 5). The additional terms in DEN are due to the feedback loops. These terms can be found by carrying out the following steps.

*Step 1. Determine the number of additional terms in DEN*

To do this, we first consider each feedback loop in the pathway separately, and count the number of enzymes which lie downstream from that feedback loop. Next we locate each pair of non-overlapping feedback loops, if there are any. For every pair present, consider the loop which is closer to the product end of the pathway (i.e., farther downstream) and count the number of enzymes which lie downstream of this feedback loop. The number of additional terms in DEN is equal to the sum total of the 'downstream' enzymes counted above.

In pathway E, note that there is *one* enzyme ($E_6$) downstream from each of the feedback loops (a) and (b); there are *two* enzymes ($E_5$ and $E_6$) downstream of the feedback loop (c), and there are *four* enzymes ($E_3$, $E_4$, $E_5$ and $E_6$) located downstream of the loop (d). Furthermore, the feedback loops (b) and (d) are non-overlapping and only *one* enzyme ($E_6$) lies downstream of the loop (b) which is closer to the product end of the pathway. Similarly, of the two non-overlapping loops, (c) and (d), the former is closer to the product end, and there are *two* enzymes ($E_5$ and $E_6$) downstream of this feedback loop. As a result, there will be a total of $1 + 1 + 2 + 4 + 1 + 2 = 11$ terms in DEN, in addition to $\Delta^0$.

*Step 2. Determine the magnitudes of the additional terms in DEN*

For this purpose, we decompose the original pathway into several component pathways. The number of

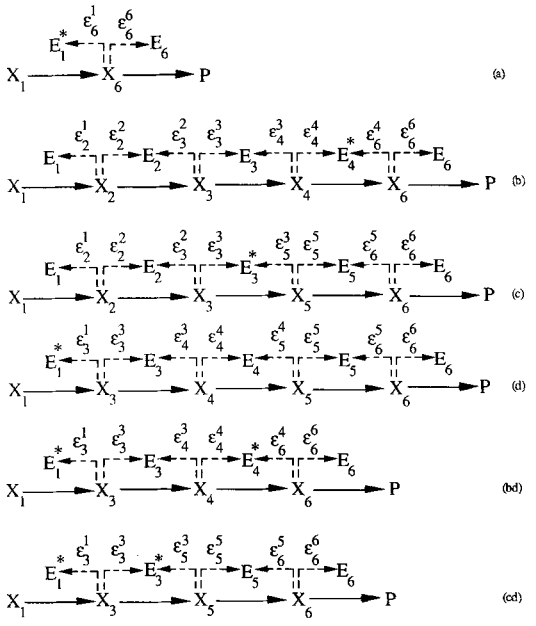

Scheme E1

component pathways is equal to the number of individual feedback loops plus the number of pairs of non-overlapping feedback loops in the original pathway. First we consider the individual feedback loops one at a time (i.e., ignore the others) and redraw the original pathway by deleting the feedback loop under consideration and all the enzymes and metabolites which lie inside the loop. We then consider each non-overlapping pair of feedback loops separately and redraw the original pathway by deleting the feedback loops and all the enzymes and metabolites located inside each loop.

The first four representations given above correspond to the feedback loops (a), (b), (c) and (d), respectively, in pathway E. The last two representations apply to the non-overlapping pairs of loops (b) and (d), and (c) and (d) in this pathway. In each representation, the enzyme(s) undergoing feedback inhibition is marked with an asterisk. For convenience of calculation, the elasticity coefficients of the various enzymes, including those due to feedback inhibition, are displayed explicitly in each representation by broken lines. (Scheme E1).

From these representations the additional terms in DEN can be readily obtained. Consider first the representations (a) through (d), in which we shall call the enzyme marked with an asterisk, a *target* enzyme. In any of these pathways, suppose that there are $n$ enzymes downstream from the target enzyme and that there are no enzymes upstream. This is the situation, for example, in the representations (a) and (d). The corresponding $n$ terms in DEN can be written down as follows. The first term is simply equal to the ratio of the magnitudes of the elasticity coefficients of the target enzyme and the enzyme immediately downstream, with respect to their adjoining metabolite. The second term is the product of the first term and the ratio of the magnitudes of the elasticity coefficients of the succeeding pair of contiguous enzymes. The third term is the product of the second term and the ratio of the magnitudes of the elasticity coefficients of the next adjacent pair of enzymes, and so on.

Consider now the situation when there are $n$ enzymes downstream from the target enzyme and there are also some enzymes upstream from it, as in the representations (b) and (c). In this case, the $n$ additional terms in DEN are formed in the same manner as described in the preceding paragraph except that now each term should be multiplied by the product of the ratios of the magnitudes of the elasticity coefficients of all consecutive pairs of enzymes (with respect to their adjoining metabolites) which lie upstream from the target enzyme.

Next we turn to the effects of the non-overlapping pairs of feedback loops and consider the representations (bd) and (cd) in Scheme E1. In these representations, of the two enzymes marked with asterisks, the enzyme located farther downstream is looked upon as the target enzyme. Suppose that there are $p$ enzymes located downstream from this target enzyme, and there are possibly some enzymes upstream. As indicated in Step 1, this situation will lead to $p$ additional terms in DEN. To find these terms, we form the product of the ratios of the magnitudes of the elasticity coefficients of all consecutive pairs of enzymes (with respect to their adjoining metabolites), which lie upstream of the target enzyme. The first of the $p$ terms is obtained by multiplying the product just formed with the ratio of the magnitudes of the elasticity coefficients of the target enzyme and the enzyme lying immediately downstream. The second term is equal to the product of the first term and the ratio of the magnitudes of the elasticity coefficients of the next adjacent pair of enzymes which are located downstream of the target enzyme, and so on.

From the above representations, the additional terms in DEN are found to be

$$\Delta_a = \frac{\bar{\varepsilon}_6^1}{\epsilon_6^6},\ \Delta_b = \frac{\bar{\varepsilon}_2^1\bar{\varepsilon}_3^2\bar{\varepsilon}_4^3\bar{\varepsilon}_6^4}{\varepsilon_2^2\varepsilon_3^3\varepsilon_4^4\varepsilon_6^6},\ \Delta_c = \frac{\bar{\varepsilon}_2^1\bar{\varepsilon}_3^2\bar{\varepsilon}_5^3}{\varepsilon_2^2\varepsilon_3^3\varepsilon_5^5} + \frac{\bar{\varepsilon}_2^1\bar{\varepsilon}_3^2\bar{\varepsilon}_5^3\bar{\varepsilon}_6^5}{\varepsilon_2^2\varepsilon_3^3\varepsilon_5^5\varepsilon_6^6}. \tag{13a}$$

$$\Delta_d = \frac{\bar{\varepsilon}_3^1}{\varepsilon_3^3} + \frac{\bar{\varepsilon}_3^1\bar{\varepsilon}_4^3}{\varepsilon_3^3\varepsilon_4^4} + \frac{\bar{\varepsilon}_3^1\bar{\varepsilon}_4^3\bar{\varepsilon}_5^4}{\varepsilon_3^3\varepsilon_4^4\varepsilon_5^5} + \frac{\bar{\varepsilon}_3^1\bar{\varepsilon}_4^3\bar{\varepsilon}_5^4\bar{\varepsilon}_6^5}{\varepsilon_3^3\varepsilon_4^4\varepsilon_5^5\varepsilon_6^6}, \tag{13b}$$

$$\Delta_{bd} = \frac{\bar{\varepsilon}_3^1\bar{\varepsilon}_4^3\bar{\varepsilon}_6^4}{\varepsilon_3^3\varepsilon_4^4\varepsilon_6^6},\ \Delta_{cd} = \frac{\bar{\varepsilon}_3^1\bar{\varepsilon}_5^3}{\varepsilon_3^3\varepsilon_5^5} + \frac{\bar{\varepsilon}_3^1\bar{\varepsilon}_5^3\bar{\varepsilon}_6^5}{\varepsilon_3^3\varepsilon_5^5\varepsilon_6^6}. \tag{13c}$$

Here the subscript on $\Delta$ refers to the representation from which the 'additional' terms are obtained. Ac-

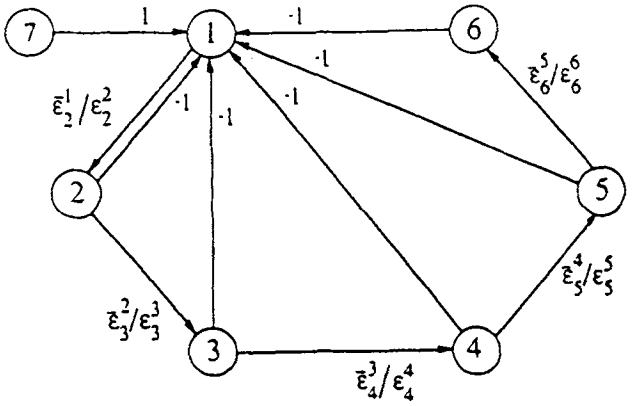


Figure 1

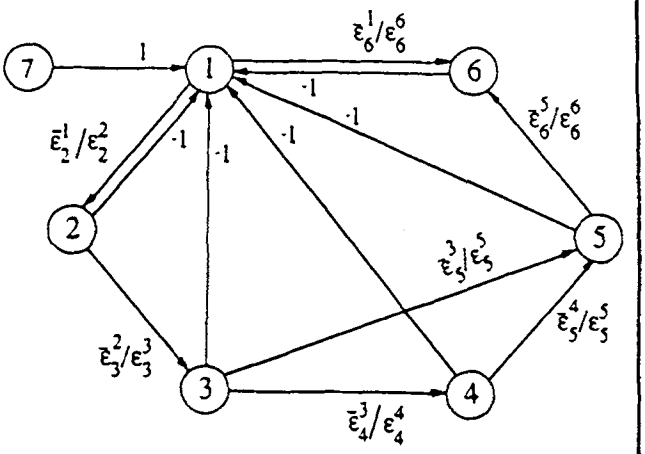


Figure 2

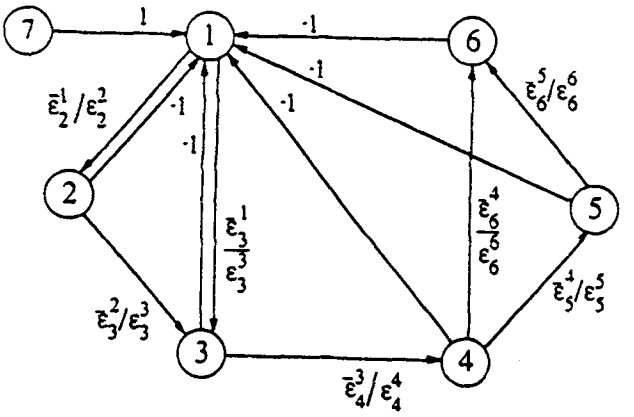


Figure 3

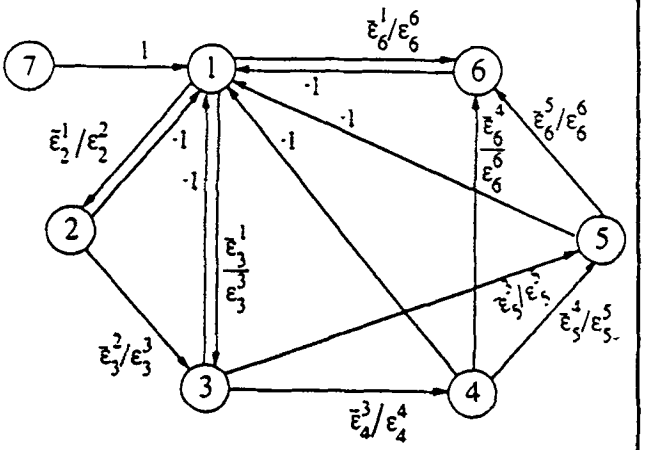


Figure 4

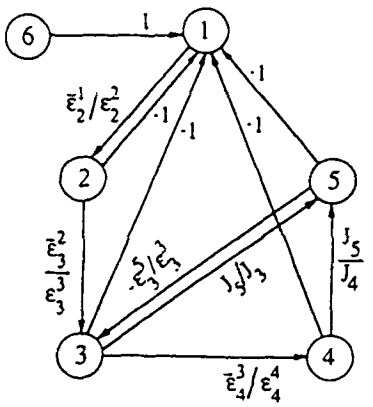


Figure 5

cordingly, the denominator DEN in Eqn. 12 is expressed as

$$\Delta^* = \Delta^0 + \Delta_a + \Delta_b + \Delta_c + \Delta_d + \Delta_{bd} + \Delta_{cd}. \quad (14)$$

It should be emphasized that with a little experience, the expressions given in Eqn 13 can be written down directly from the topology of the feedback loops in the original pathway E, and it is not necessary to draw the representations (a)–(d), (bd) and (cd), explicitly.

The numerator NUM in Eqn. 12 can also be obtained using a superposition technique. We may write: NUM = $\Delta_{i-1}$ + regulatory terms, where $\Delta_{i-1}$ is the numerator in the expression for $C_i^J$ ($i = 1, 2, 3, 4, 5, 6$) in the unregulated pathway (with $\Delta_0 = 1$), and the regulatory terms represent the contribution from the feedback loops. We now describe how to calculate these regulatory terms.

*Step 3. Determine the number of regulatory terms in NUM*

To determine the number of regulatory terms in the numerator of $C_i^J$, we examine the location of the enzyme $E_i$ with respect to the position of the individual feedback loops in the original pathway. If $E_i$ does not lie downstream of a particular feedback loop, then there will be no regulatory terms in NUM due to that feedback loop. If, on the other hand, $E_i$ is located downstream from a feedback loop, then that feedback loop will contribute a regulatory term in NUM of $C_i^J$. Furthermore, when there is a pair of non-overlapping feedback loops located upstream of the enzyme $E_i$, an additional regulatory term will result in NUM.

*Step 4. Determine the magnitudes of the regulatory terms in NUM*

It was indicated in Step 3 that if an enzyme $E_i$ does not lie downstream of any of the feedback loops in the pathway, then there will be no regulatory terms in NUM; in other words, NUM will simply be equal to $\Delta_{i-1}$, its value for the unregulated pathway. In pathway E, note that there are no feedback loops upstream from the enzyme $E_1$ or $E_2$. Therefore, the flux control coefficients of these two enzymes are given by: $C_1^J = 1/\Delta^*$, and $C_2^J = \Delta_1/\Delta^*$.

Let us now consider an enzyme $E_i$, which is located downstream from a feedback loop in the original pathway. Ignoring the presence of the other feedback loops, we represent this pathway (with the one feedback loop) in the manner described in Step 2 above (i.e., delete the feedback loop and all its intervening enzymes and metabolites) but terminate the pathway at the enzyme $E_i$ (and the metabolite $X_i$). The contribution of this feedback loop in NUM of $C_i^J$ is obtained by forming the product of the ratio of the magnitudes of the elasticity coefficients of each consecutive pair of enzymes in the 'reduced' pathway. This process should be repeated for each individual feedback loop which is present in the original pathway. Furthermore, if there are two non-overlapping feedback loops upstream from the enzyme $E_i$, an additional term must be included in NUM. The magnitude of this additional term is found by constructing a reduced pathway in the manner just described (i.e. by deleting both feedback loops and the enzymes and metabolites intervening each loop, and terminating the resulting pathway at the enzyme $E_i$) and subsequently forming the product of the ratios of the magnitudes of the appropriate elasticity coefficients.

Note that in pathway E, the enzyme $E_3$ is situated downstream from the feedback loop (d) only. In this case, the reduced pathway is given by the representation (d) terminated after the enzyme $E_3$ (and the metabolite $X_3$). From this reduced pathway, we find that the only regulatory term in NUM of $C_3^J$ is equal to $\bar{\varepsilon}_3^1/\varepsilon_3^3$ so that

$$C_3^J = \frac{1}{\Delta^*}\left[\Delta_2 + \frac{\bar{\varepsilon}_3^1}{\varepsilon_3^3}\right]. \quad (15)$$

Similarly, since the enzyme $E_4$ lies downstream only from the feedback loop (d) in pathway E, the corresponding reduced pathway is given by the representation (d), which is now terminated after this enzyme (and the metabolite $X_4$). If follows that

$$C_4^J = \frac{1}{\Delta^*}\left[\Delta_3 + \frac{\bar{\varepsilon}_3^1\bar{\varepsilon}_4^3}{\varepsilon_3^3\varepsilon_4^4}\right]. \quad (16)$$

To calculate $C_5^J$, notice that the enzyme $E_5$ is located downstream from the feedback loops (c) and (d) in pathway E. The corresponding reduced pathways are given by the representations (c) and (d), each truncated after the enzyme $E_5$ (and the metabolite $X_5$). Furthermore, since these two feedback loops do not overlap in the original pathway, we must consider another reduced pathway, which is obtained from the representation (cd) terminated at the enzyme $E_5$ (and the metabolite $X_5$). From these reduced pathways, we find

Fig. 1. A signal flow graph for the control structure of the unregulated pathway A.
Fig. 2. A signal flow graph for pathway B.
Fig. 3. A signal flow graph for pathway C.
Fig. 4. A signal flow graph for pathway E.
Fig. 5. A signal flow graph for the branched pathway F.

$$C_5^J = \frac{1}{\Delta^*}\left[\Delta_4 + \frac{\bar{\varepsilon}_3^1\bar{\varepsilon}_4^3\bar{\varepsilon}_5^4}{\varepsilon_3^3\varepsilon_4^4\varepsilon_5^5} + \frac{\bar{\varepsilon}_2^1\bar{\varepsilon}_3^2\bar{\varepsilon}_5^3}{\varepsilon_2^2\varepsilon_3^3\varepsilon_5^5} + \frac{\bar{\varepsilon}_3^1\bar{\varepsilon}_5^3}{\varepsilon_3^3\varepsilon_5^5}\right]. \tag{17}$$

Finally, observe that in pathway E, the enzyme $E_6$ is located downstream from each of the four feedback loops (a)–(d), and there are also two non-overlapping pairs of feedback loops, (b) and (d), and (c) and (d), upstream from this enzyme. In view of this, the reduced pathways for this case are the same as the representations (a)–(d), (bd) and (cd). These representations yield the following expression for $C_6^J$.

$$C_6^J = \frac{1}{\Delta^*}\left[\Delta_5 + \frac{\bar{\varepsilon}_6^1}{\varepsilon_6^6} + \frac{\bar{\varepsilon}_2^1\bar{\varepsilon}_3^2\bar{\varepsilon}_4^3\bar{\varepsilon}_6^4}{\varepsilon_2^2\varepsilon_3^3\varepsilon_4^4\varepsilon_6^6} + \frac{\bar{\varepsilon}_2^1\bar{\varepsilon}_3^2\bar{\varepsilon}_5^3\bar{\varepsilon}_6^5}{\varepsilon_2^2\varepsilon_3^3\varepsilon_5^5\varepsilon_6^6} + \frac{\bar{\varepsilon}_3^1\bar{\varepsilon}_4^3\bar{\varepsilon}_5^4\bar{\varepsilon}_6^5}{\varepsilon_3^3\varepsilon_4^4\varepsilon_5^5\varepsilon_6^6} + \frac{\bar{\varepsilon}_3^1\bar{\varepsilon}_4^3\bar{\varepsilon}_6^4}{\varepsilon_3^3\varepsilon_4^4\varepsilon_6^6} + \frac{\bar{\varepsilon}_3^1\bar{\varepsilon}_5^3\bar{\varepsilon}_6^5}{\varepsilon_3^3\varepsilon_5^5\varepsilon_6^6}\right]. \tag{18}$$

It should be pointed out that the sum total of the regulatory terms in the numerators (NUM) of *all* the flux control coefficients is the same as the sum of the additional terms in the denominator (DEN). Thus, in actual computation, it it not necessary to find the additional terms in DEN by carrying out steps 1 and 2; they can be obtained by first finding the additional terms in NUM of the flux control coefficient of each of the enzymes using steps 3 and 4, and subsequently forming their sum. For completeness, the signal flow graph of this pathway is presented in Fig. 4, from which the above results can be readily verified.

The foregoing discussion is confined to linear metabolic pathways with a pattern of two non-overlapping feedback loops. It is apparent that the present methodology can be easily extended if the pathway contains a pattern of three or more non-overlapping feedback loops. However, for the sake of brevity, these ramifications will not be treated here.

## Control analysis of branched pathways

In a linear metabolic pathway the control coefficients of the enzymes depend only on their elasticity coefficients. The control coefficients of the enzymes in a branched pathway, on the other hand, depend also on the fluxes through the different branches. We will show below how these fluxes can be incorporated into a signal flow graph from which the flux control coefficients of the enzymes are evaluated. We will also describe a systematic procedure for converting a signal flow graph to a simpler from which may significantly reduce the effort necessary for calculating the flux control coefficients. Modifications of a signal flow graph

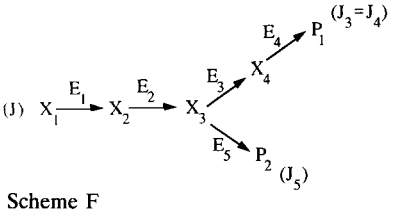


Scheme F

for determining the relative proportions of flux control of the various enzyme are also discussed.

For the present purpose, we consider a simple branched pathway (Scheme F) consisting of five enzymes, $E_1$ through $E_5$, and three variable metabolites $X_2$, $X_3$ and $X_4$. The metabolite $X_1$ represents the initial substrate, and $P_1$ and $P_2$ are the final products. It is assumed that $X_1$, $P_1$ and $P_2$ are maintained at constant concentration levels. The fluxes through the various linear segments of the pathway are shown inside parantheses. Note that $J_3 = J_4 = J - J_5$. Here we will deal only with the flux control coefficients. It should be pointed out, however, that a similar methodology can be employed for evaluating the concentration control coefficients (see, for example, Ref. 4).

*Construction of a signal flow graph*

For the present analysis we shall define the flux control coefficients of the enzymes with reference to the flux $J$. Mathematically, the flux control coefficient of an enzyme $E_i$, when referred to this flux, is given by

$$C_i^J = \frac{e_i}{J}\frac{\partial J}{\partial e_i}, \tag{19}$$

$e_i$ being the concentration of the enzyme. Here the superscript $J$ indicates that it has been used as the reference flux. As with linear pathways, a signal flow graph for the control structure of a branched pathway can be constructed directly from the reaction pattern of the pathway, without the necessity of writing down the governing equations (i.e., summation and connectivity theorems, and branch point relationships) explicitly. The foundation of this heuristic procedure is discussed in Appendix A using a matrix formulation. To begin with, we redraw the pathway displaying all the elasticity coefficients (Scheme F1). As usual, the elasticity coefficient ($\varepsilon_j^i$) of an enzyme $E_i$ with respect to a metabolite $X_j$ is shown by a dotted line pointing from

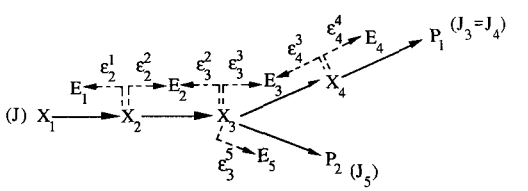


Scheme F1

the metabolite to the enzyme. From the representation in Scheme F1, a signal flow graph can be constructed in several ways. One such procedure is described in this section, and an alternate strategy is discussed in Appendix B. First we treat the initial-substrate containing segment and the upper branch of the pathway F as a linear pathway and draw its signal flow graph (without a source node). Effects of the various fluxes and the lower branch are subsequently incorporated into this signal flow graph. For this purpose we draw the nodes 1–4 representing the enzymes $E_1$–$E_4$ and their unknown flux control coefficients (see Fig. 5). A directed edge is then drawn from node $i$ to node $i+1$, $i = 1, 2, 3$. The weight on the edge $(i, i+1)$ is taken equal to the *signed* ratio of the elasticity coefficients of the enzymes $E_i$ and $E_{i+1}$ with respect to their common metabolite $X_{i+1}$. The sign of this ratio is fixed by using the following convention (see Ref. 4). In this 'linear' segment of pathway F1, if an elasticity coefficient points in the forward (i.e., downstream) direction, then it is used without a change of sign; if, on the other hand, an elasticity coefficient points in the reverse (i.e., upstream) direction, then it is used with its sign reversed. Furthermore, an elasticity coefficient, $\varepsilon_j^i$, due to product inhibition, is written as $\varepsilon_j^i = -\bar{\varepsilon}_j^i$, $\bar{\varepsilon}_j^i$ being the absolute magnitude of $\varepsilon_j^i$. Next an edge of weight $-1$ is directed from the nodes 2, 3 and 4 to node 1. We now take into account the various fluxes and the lower branch. The flux control coefficient of the only enzyme $E_5$ in the lower branch is designated by node 5 and an edge of weight $-1$ is directed from this node to node 1, in keeping with the summation theorem for the entire pathway F. To accommodate the elasticity coefficient of this enzyme into the signal flow graph, we focus our attention at the branch point. In particular, consider the enzymes $E_5$ and $E_3$ as contiguous enzymes with $X_3$ as the adjoining metabolite and draw a directed edge from node 5 to node 3 carrying a weight $-\varepsilon_3^5/\varepsilon_3^3$, which is equal to the *negative* of the ratio of the elasticity coefficients of the enzymes $E_5$ and $E_3$ with respect to the metabolite $X_3$. Finally an edge is directed from each of the nodes 3 and 4 (corresponding to the enzymes $E_3$ and $E_4$ in the upper branch) to node 5. These edges carry the weights equal to the ratios $J_5/J_3$ and $J_5/J_4$ of the fluxes through the upper and lower branches (recall that $J_3 = J_4$). To complete our construction, a source node (i.e., node 6) is introduced and an edge of weight unity is directed from the source node to node 1. It should be mentioned that in the foregoing procedure, the initial-substrate containing segment and the upper branch are treated as a linear pathway solely for the purpose of constructing a signal flow graph, although the fluxes transmitted through the two segments are different.

We should point out that the governing equations, namely, the summation and connectivity theorems and branch point relationships can be easily produced from the signal flow graph. For instance, the summation theorem can be obtained as follows. Form the product of the weight of each incoming edge of node 1 and the flux control coefficient associated with the node from which the edge emanates. (The source node is assigned a fictitious flux control coefficient of unity). If the sum of these products is added to the negative of the flux control coefficient of node 1 and equated to zero, the summation theorem results: $C_1^J + C_2^J + C_3^J + C_4^J + C_5^J = 1$. The connectivity theorems can be derived in an analogous fashion by considering the nodes 2, 3 and 4. To generate the branch point relationship, we apply the above procedure at node 5 (see Eqn. A-1 in Appendix A).

An alternate strategy for drawing a signal flow graph for this pathway is to treat the segment containing the enzymes $E_1$, $E_2$ and $E_5$ as a linear pathway and draw its signal flow graph; effects of the various fluxes and the enzymes in the upper branch are subsequently incorporated into the signal flow graph. The details of this procedure are given in Appendix B. In Appendix C, we describe a systematic procedure for constructing a signal flow graph for a branched pathway which may contain any number of enzymes in each of its segments. Based on the results obtained from the signal flow graphs, a heuristic method is presented for calculating the flux control coefficients of the enzymes directly from the reaction sequence of the pathway (without drawing a signal flow graph).

*Evaluation of the flux control coefficients*

The flux control coefficients of the enzymes in pathway F can be derived from Fig. 5 with the aid of the formulas given by Eqns. 1 and 2. This is done as follows. Note that there are seven first-order cycles in this figure; these are illustrated in Fig. 6. There are also two second-order cycles in Fig. 5, as depicted in Fig. 7. With the gains of these nine cycles, we find from Eqn. 2:

$$\Delta^\dagger = 1 + \frac{\bar{\varepsilon}_2^1}{\varepsilon_2^2} + \frac{\bar{\varepsilon}_2^1\bar{\varepsilon}_3^2}{\varepsilon_3^2\varepsilon_3^3} + \frac{\bar{\varepsilon}_2^1\bar{\varepsilon}_3^2\bar{\varepsilon}_4^3}{\varepsilon_2^2\varepsilon_3^3\varepsilon_4^4}\frac{J_5}{J_4} + \frac{\varepsilon_3^5}{\varepsilon_3^3}\frac{J_5}{J_3} + \frac{\varepsilon_3^5\bar{\varepsilon}_4^3}{\varepsilon_3^3\varepsilon_4^4}\frac{J_5}{J_4}$$

$$+ \frac{\bar{\varepsilon}_2^1\bar{\varepsilon}_3^2}{\varepsilon_2^2\varepsilon_3^3}\frac{J_5}{J_3} + \frac{\bar{\varepsilon}_2^1\varepsilon_3^5}{\varepsilon_2^2\varepsilon_3^3}\frac{J_5}{J_3} + \frac{\bar{\varepsilon}_2^1\varepsilon_3^5\bar{\varepsilon}_4^3}{\varepsilon_2^2\varepsilon_3^3\varepsilon_4^4}\frac{J_5}{J_4}. \qquad (20)$$

The superscript † has been used here to indicate that it applies to the branched pathway, F. As an example, we now calculate the flux control coefficient of the first enzyme. In Fig. 5, observe that there is only one direct path from the source node to node 1. The gain of this directed path is unity. In Eqn. 1, we therefore have $i = 1$, $k = 1$ and $G_{11} = 1$. In relation to this directed path, there are two nontouching cycles in Fig. 5; these are given in Fig. 6 (v) and (vi). Using the gains of these

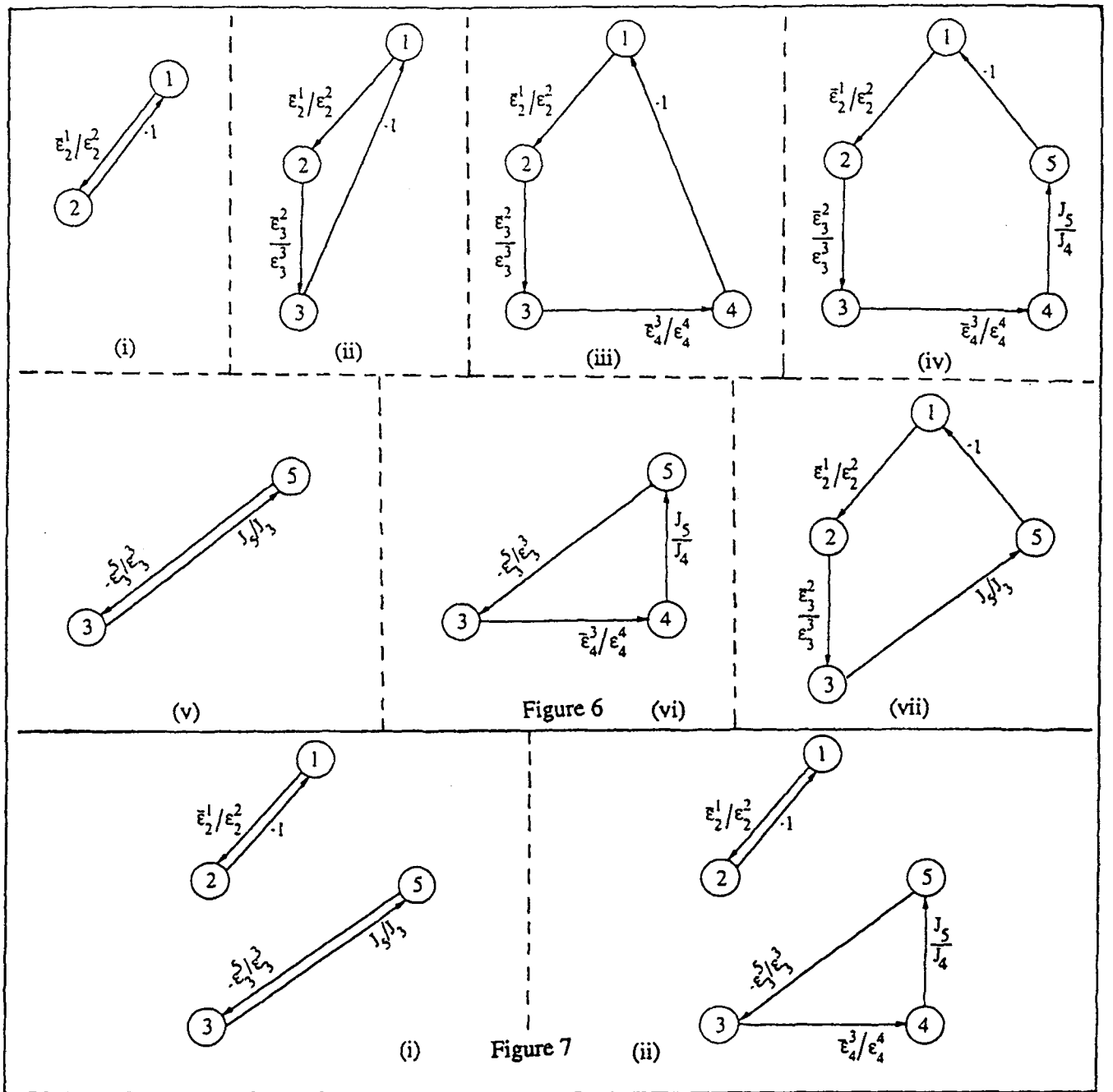


Figure 6




Figure 7

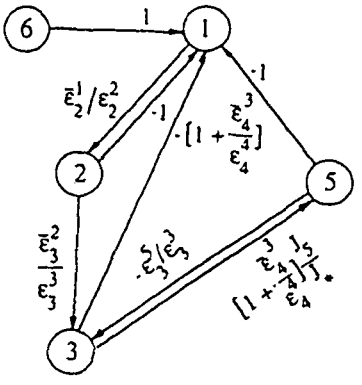

Figure 8

nontouching cycles from the expression for $\Delta^\dagger$ (including the first term of 1) and the fact that $G_{11} = 1$, we obtained from Eqn. 1 the following expression for $C_1^J$.

$$C_1^J = \left[1 + \frac{\varepsilon_3^5}{\varepsilon_3^3}\left(1 + \frac{\bar{\varepsilon}_4^3}{\varepsilon_4^4}\right)\frac{J_5}{J_*}\right]/\Delta^\dagger. \tag{21}$$

Here we have written $J_3 = J_4 = J_*$. As another example, let us evaluate $C_3^J$. Clearly, there is a directed path from the source node to node 3 in Fig. 5, with a gain of $\bar{\varepsilon}_2^1\bar{\varepsilon}_3^2/(\varepsilon_2^2\varepsilon_3^3)$. Since each of the cycles shown in Fig. 6 touches this directed path, it follows that

$$C_3^J = \frac{\bar{\varepsilon}_2^1\bar{\varepsilon}_3^2}{\varepsilon_2^2\varepsilon_3^3}/\Delta^\dagger. \tag{22}$$

Expressions for the remaining flux control coefficients can be derived in a similar fashion. Whenever possible, advantage should also be taken of the simplicity of a node in the signal flow graph. Consider, for definiteness, node 2 in Fig. 5. This node is *simple* in the sense that it has only one incoming edge. As a consequence, we have the relationship $(\bar{\varepsilon}_2^1/\varepsilon_2^2)C_1^J - C_2^J = 0$, which is in fact the connectivity theorem for the enzymes $E_2$ and $E_2$. Therefore, once $C_1^J$ is found from the signal flow graph, as given by Eqn. 21, the expression for $C_2^J$ can be easily deduced. Similarly, using the relation $(\bar{\varepsilon}_4^3/\varepsilon_4^4)C_3^J - C_4^J = 0$, at node 4 and the result given by Eqn. 22, $C_4^J$ can be readily evaluated.

Calculation of the flux control coefficients from Eqns. 1 and 2 can be considerably simplified by writing these equations in the form

$$C_i^J = N_i / \sum_{r=1}^{5} N_r,$$

where $N_i = \Sigma_k G_{ki} R_{ki}$, $G_{ki}$ being the gain of the $k$-th directed path from the source node to node $i$ in the signal flow graph, and $R_{ki} = 1 - L_{ik} + L_{2k} - \ldots$, $L_{ik}$, $L_{2k}, \ldots$ are each the sum of the gains of the first-order, second-order cycles, etc. which do not touch the $k$-th directed path from the source node to node $i$. The main advantage of this formulation is that it avoids locating *all* the cycles in the signal flow graph at once in order to evaluate $\Delta$ in Eqn. 1.

As an example, if we want to calculate $N_1$ (for $C_1^J$) from the signal flow graph of Fig. 5, we simply locate all the directed paths from the source node to node 1 in this figure and the first order, second order cycles, etc. which do not touch each of these directed paths. Clearly there is only one directed path from the source node to node 1 in Fig. 5 and there are two nontouching first order cycles; see Fig. 6 (v) and (vi). From the gains of this directed path and the nontouching cycles, it follows that $N_1$ is given by the numerator on the right hand side of Eqn. 21.

*Reduction of a signal flow graph*

We will now describe a systematic procedure by which the topological structure of a signal flow graph can be simplified in order to reduce the effort necessary for the evaluation of the control coefficients. The procedure consists of eliminating the appropriate node(s) from the signal flow graph. By a judicious choice of the nodes to be eliminated, a significant reduction in time and effort can be achieved. We will illustrate the node elimination process in connection with the signal flow graph shown in Fig. 5. It is convenient to eliminate a node with a simpler structure, i.e. which has fewer edges connected to it. In Fig. 5, node 2 and node 4 are two such nodes. First, we will eliminate node 4 from Fig. 5 and investigate the degree of simplification. In general, consider an arbitrary node $k$, which is to be eliminated from a signal flow graph. Suppose that there are two other nodes $i$ and $j$ such that there is a directed edge of weight $w_{ik}$ from node $i$ to node $k$, and a directed edge from node $k$ to node $j$ of weight $w_{kj}$. To eliminate node $k$, we simply draw a directed edge from node $i$ to node $j$ and attach to it a weight $c_{ij}$ which is equal to the product $w_{ik}w_{kj}$. If a directed edge from node $i$ to node $j$ is originally present in the signal flow graph, say, with a weight $w_{ij}$, then we replace the weight $w_{ij}$ by $(w_{ij} + c_{ij})$. The node $k$ and all its incoming and outgoing edges are subsequently deleted from the signal flow graph. It should be emphasized that the above procedure must be carried out for *each* pair of nodes $i$ and $j$ which are connected to the node $k$, to be eliminated. In relation to node 4 in Fig. 5, there are two such pairs of nodes; these are nodes 3 and 5, and nodes 3 and 1. By performing the foregoing operations, node 4 is eliminated from Fig. 5, leading to the signal flow graph of Fig. 8. In this figure, the fluxes $J_3$ and $J_4$, which are equal, are written as $J_*$. It is apparent that in Fig. 8 there are only four first-order cycles and one second-order cycle, in contrast with seven first-order and two second-order cycles in Fig. 5. In other words, the topological structure of the signal flow graph of Fig. 5 has been significantly reduced. Fig. 9(i)–(iii) depicts three of the four first-order cycles present in Fig. 8; the remaining first-order cycle was shown earlier in Fig. 6(i); the only second-order cycle in Fig. 8 is displayed in Fig. 9(iv). Collecting the gains of these loops, the

Fig. 6. The seven first-order cycles in the signal flow graph of Fig. 5.
Fig. 7. The two second-order cycles in the signal flow graph of Fig. 5.
Fig. 8. The signal flow graph of Fig. 5 after elimination of node 4.

denominator on the right hand side of Eqn. 1, which is now denoted by $\tilde{\Delta}$, is found to be

$$\tilde{\Delta} = 1 + \frac{\bar{\varepsilon}_2^1}{\varepsilon_2^2} + \frac{\bar{\varepsilon}_2^1 \bar{\varepsilon}_3^2}{\varepsilon_2^2 \varepsilon_3^3}\left(1 + \frac{\bar{\varepsilon}_4^3}{\varepsilon_4^4}\right) + \frac{\bar{\varepsilon}_2^1 \bar{\varepsilon}_3^2}{\varepsilon_2^2 \varepsilon_3^3}\left(1 + \frac{\bar{\varepsilon}_4^3}{\varepsilon_4^4}\right)\frac{J_5}{J_*} + \frac{\varepsilon_3^5}{\varepsilon_3^3}\left(1 + \frac{\bar{\varepsilon}_4^3}{\varepsilon_4^4}\right)\frac{J_5}{J_*}$$

$$+ \frac{\bar{\varepsilon}_2^1 \varepsilon_3^5}{\varepsilon_2^2 \varepsilon_3^3}\left(1 + \frac{\bar{\varepsilon}_4^3}{\varepsilon_4^4}\right)\frac{J_5}{J_*}. \qquad (23)$$

This result is identical with the expression for $\Delta^\dagger$ given in Eqn. 20. The flux control coefficients $C_i^J$ ($i = 1, 2, 3$ and 5) can be deduced by examining the directed path from the source node to the respective node and the nontouching cycles (if any) in Fig. 8. It is not difficult to see that these considerations yield the same results for the flux control coefficients as those obtained earlier from Fig. 5. Once $C_3^J$ is found, $C_4^J$ can be derived

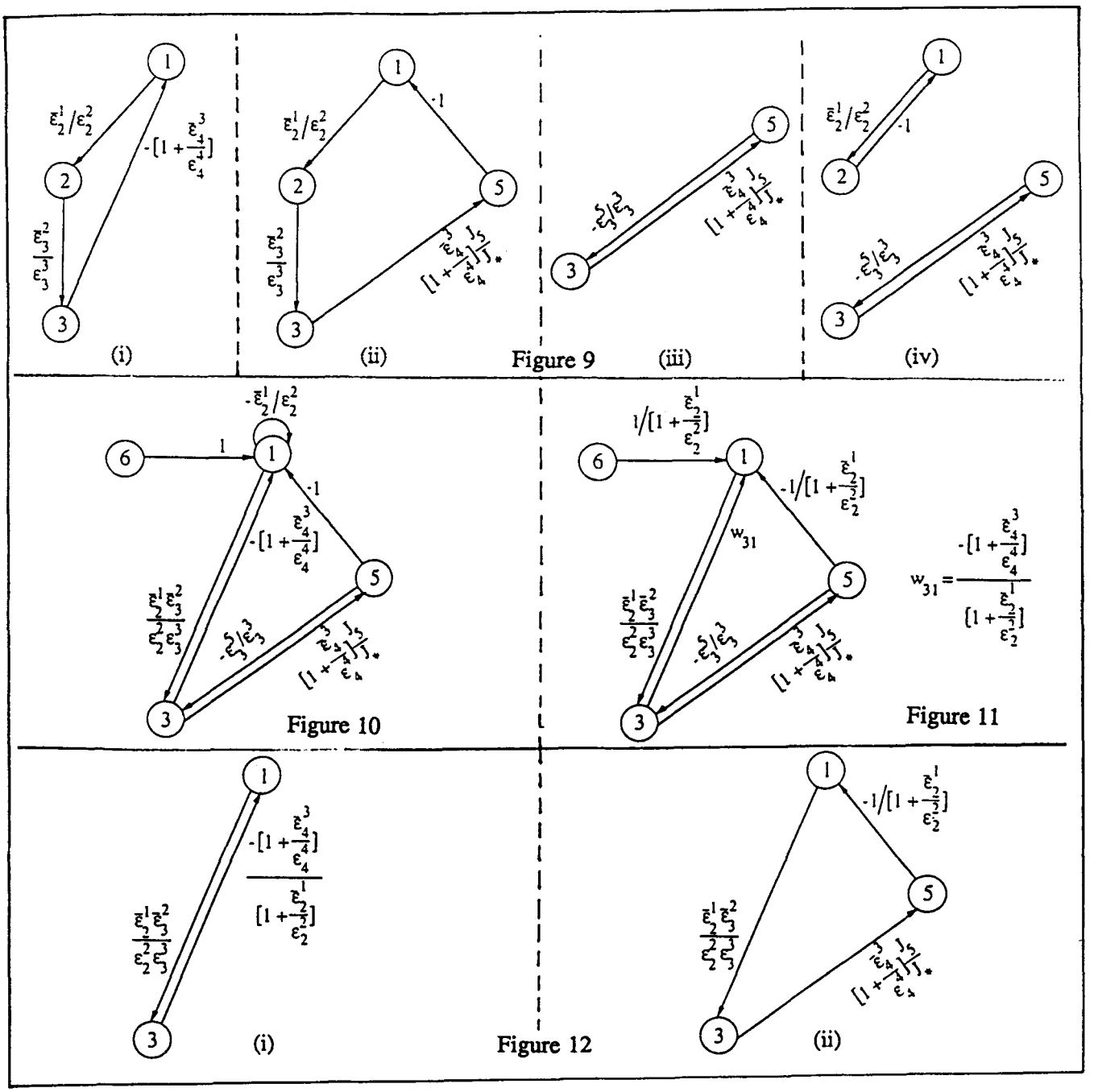


Fig. 9. Three of the four first-order cycles in Fig. 8 are shown in parts (i)–(iii) and the remaining first order cycle is given in Fig. 6(i); part (iv) of this figure depicts the only second order cycle present in Fig. 8.

Fig. 10. Signal flow graph of Fig. 9 after elimination of node 2. Note that a cycle is created around node 1.

Fig. 11. Signal flow graph of Fig. 10 after elimination of the cycle around node 1.

Fig. 12. Two of the three first-order cycles in Fig. 11; the other first-order cycle is given in Fig. 9(iii).

with the aid of the relation $(\bar{\varepsilon}_4^3/\varepsilon_4^4)C_3^J - C_4^J = 0$, which applies at the *simple* node 4, as shown before.

A further simplification can be made by eliminating node 2 from Fig. 8. Note that node 2 is connected to the nodes 1 and 3 by the edges (1,2) and (2,3); it is also connected to node 1 by the edges (1,2) and (2,1). To eliminate this node we first consider the edges (1,2) and (2,3). According to the procedure described in the preceding paragraph, we introduce a directed edge in Fig. 8 from node 1 to node 3 with a weight equal to $\bar{\varepsilon}_2^1\bar{\varepsilon}_3^2/\varepsilon_2^2\varepsilon_3^3$. Next for the pair of edges (1,2) and (2,1), we create a cycle (i.e., a self-loop) around node 1 and attach a weight $w_{11}$, equal to the product of the weights on the two edges. Node 2 and the edges (1,2), (2,1) and (2,3) are then deleted from the figure. The resulting signal flow graph is depicted in Fig. 10. The cycle around node 1 in Fig. 10 is subsequently eliminated by dividing the weight of every incoming edge of node 1 by $(1-w_{11})$, as illustrated in Fig. 11. Observe now that Fig. 11 has only three first-order cycles and no second-order cycles. Two of these first-order cycles are shown in Fig. 12; the other first order cycle was given in Fig. 9(iii). Subtracting the sum of the gains of these first order cycles from unity, it is easily seen that the result is equal to $\Delta^\dagger/(1+\bar{\varepsilon}_2^1/\varepsilon_2^2)$, where $\Delta^\dagger$ has the value given by Eqn. 20. The flux control coefficients $C_1^J$, $C_3^J$ and $C_5^J$ can be determined from Fig. 11 by examining the directed path from the source node to each of the nodes 1, 3 and 5, and the nontouching loops (if any) in regard to these directed paths. The details will not be presented here. Knowing $C_1^J$ and $C_3^J$, expressions for $C_2^J$ and $C_4^J$ can be derived by invoking the 'connectivity relationships' at the *simple* nodes 2 and 4, as discussed earlier. After gaining a little experience, this step-by-step reduction procedure can be carried out with ease, and a great deal of effort can be saved in the evaluation of the control coefficients

*Relative magnitudes of flux control*

In order to determine which of the enzymes in pathway F are most dominant in regulating the flux, it is more pragmatic to find the relative proportions of the flux control coefficients of the enzymes rather than their actual magnitudes. A signal flow graph provides a simple way of doing this. Suppose that in pathway F, we want to assess the importance of flux control of the various enzymes relative to that of the first enzyme; in order words, we want to calculate the ratio of $C_2^J$, $C_3^J$, $C_4^J$ and $C_5^J$ to $C_1^J$. As shown in Ref. 4, this can be accomplished by converting node 1 in Fig. 5 into a source node. We point out that by definition, a source node is a node from which all edges must emanate, i.e., it does not have any incoming edges. In Fig. 5, note that there is a directed edge (6,1) from node 6 to node 1 with a weight $w_{61} = 1$. To convert node 1 into a source node, we first move all the edges terminating at node 1 so that they now terminate at the original source node 6. This procedure transforms the directed edge from node 6 to node 1 into a self-loop around node 6. We move the initial node of this self-loop to node 1 and assign to it a weight equal to $1/w_{61}$, which is unity. The edge (6,1) in the original signal flow graph thus becomes the inverted edge (1,6). Next we multiply the weights of all other edges whose terminal nodes have been moved to node 6 by the factor $(-1/w_{61})$; in the present case since $w_{61} = 1$, this simply amounts to changing the signs of the weights on these edges. The resulting signal flow graph is depicted in Fig. 13. From this figure the flux control coefficient $C_p^J$ ($p = 2$, 3, 4 and 5) of an enzyme $E_p$ relative to that of the first enzyme can be obtained with the aid of the formula

$$\frac{C_p^J}{C_1^J} = \frac{1}{\Delta^{**}}\sum_k G_{k1p}^* \Delta_{k1p}^*. \tag{24}$$

Here

$$\Delta^{**} = 1 - M_1 + M_2 - M_3 + \ldots, \tag{25}$$

$M_1$ being the sum of the gains of all first-order cycles, $M_2$ the sum of the gains of all second-order cycles, etc. in Fig. 13. The symbol $G_{k1p}^*$ denotes the gain of the $k$-th directed path from node 1 to node $p$, and $\Delta_{k1p}^*$ consists of those terms in $\Delta^{**}$ (including the first term of 1) which correspond to the cycles in Fig. 13 that do not touch the $k$-th directed path from node 1 to node $p$. Fig. 13 has two first-order cycles and no second-order cycles. The first-order cycles are given in Fig. 6(v) and (vi). The sum of the gains of these first-order cycles leads to

$$\Delta^{**} = 1 + \frac{\varepsilon_3^5}{\varepsilon_3^3}\left(1 + \frac{\bar{\varepsilon}_4^3}{\varepsilon_4^4}\right)\frac{J_5}{J_*}. \tag{26}$$

We now evaluate $C_3^J/C_1^J$, as an example. In Fig. 13, since there is only one directed path from node 1 to node 3 with a gain of $\bar{\varepsilon}_2^1\bar{\varepsilon}_3^2/(\varepsilon_2^2\varepsilon_3^3)$, and all the cycles touch this directed path, it follows that

$$\frac{C_3^J}{C_1^J} = \frac{1}{\Delta^{**}}\left[\frac{\bar{\varepsilon}_2^1\bar{\varepsilon}_3^2}{\varepsilon_2^2\varepsilon_3^3}\right]. \tag{27}$$

This result is consistent with the expressions for $C_1^J$ and $C_3^J$ given in Eqns. 21 and 22. Similarly, observe that in Fig. 13 there are two directed paths from node 1 to node 5, with no nontouching cycles. Substituting the gains of these directed paths in Eqn. 24, we find

$$\frac{C_5^J}{C_1^J} = \frac{1}{\Delta^{**}}\frac{\bar{\varepsilon}_2^1\bar{\varepsilon}_3^2}{\varepsilon_2^2\varepsilon_3^3}\left(1 + \frac{\bar{\varepsilon}_4^3}{\varepsilon_4^4}\right)\frac{J_5}{J_*}. \tag{28}$$

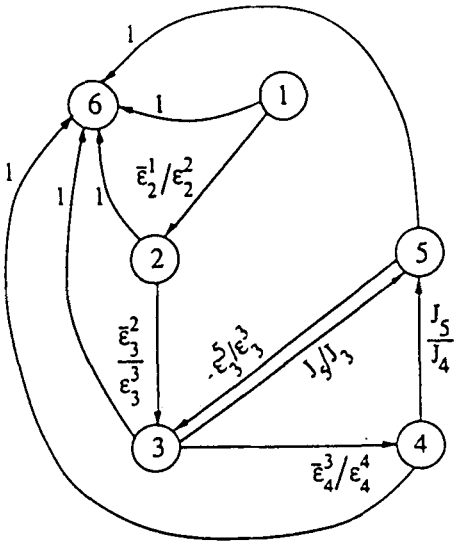


Figure 13

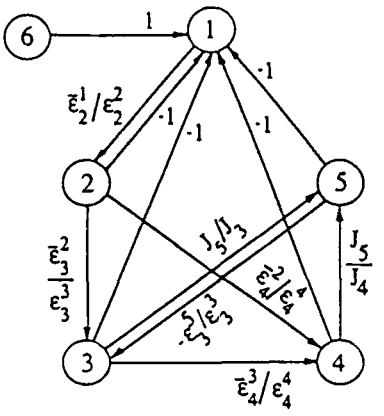


Figure 14

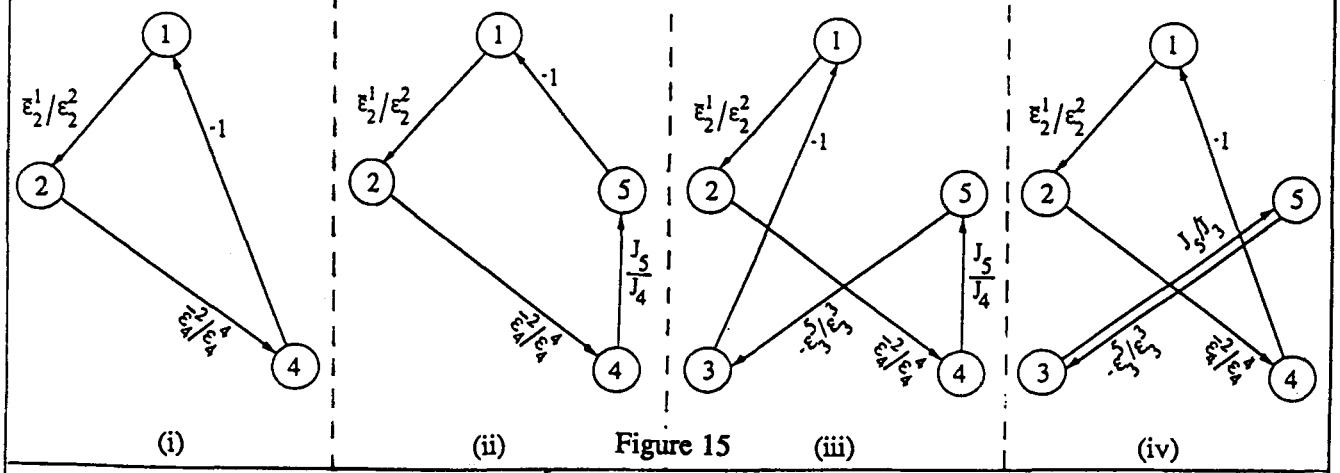


Figure 15

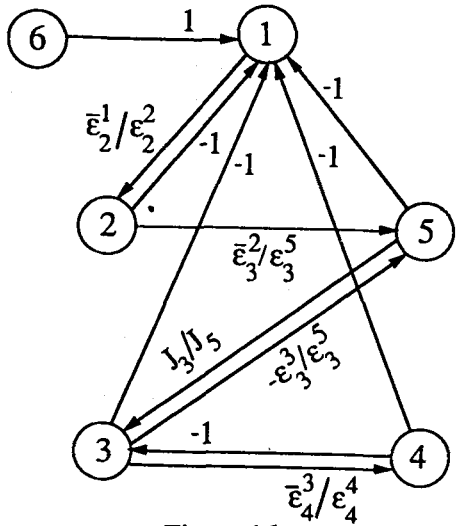


Figure 16

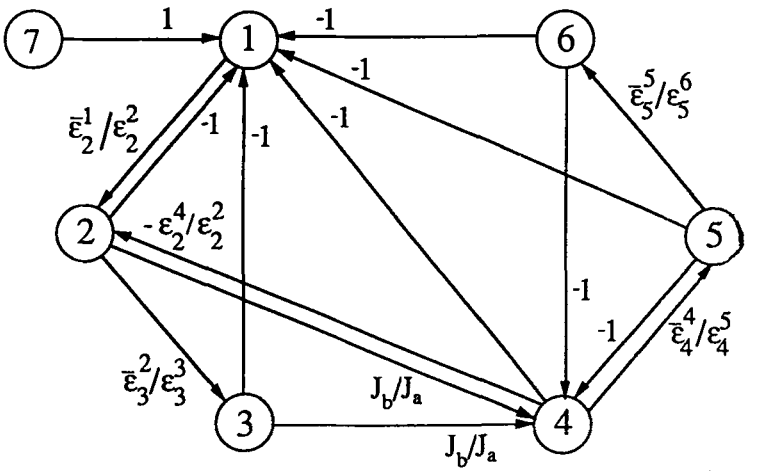


Figure 17

The other ratios can be obtained in the same manner. From these ratios the relative importance of the various enzymes in flux control can be readily assessed.

*Further results and discussion*

In the foregoing sections, the flux-control distribution in pathway F was analysed with regard to the flux $J$. It is also relevant to study the control exerted by the various enzymes in this pathway on the fluxes through the two dividing branches. For this purpose, Westerhoff and Kell [9] suggested the use of the so-called flux-branching ratio which is defined as the ratio of the fluxes in the two branches, namely, $R = J_*/J_5$. (Recall that $J_3 = J_4 = J_*$.) To describe the regulatory effects of the enzymes on this flux-branching ratio, they introduced the notion of a flux-ratio control coefficient. For an enzyme $E_i$ with concentration $e_i$, this is defined by

$$C_i^R = \frac{e_i}{R}\frac{\partial R}{\partial e_i}, \tag{29}$$

which characterizes a fractional change in the flux-branching ratio in response to a fractional change in enzyme concentration. Expressions for these flux-ratio control coefficients $C_i^R$ ($i = 1, 2, 3, 4, 5$) can be derived by modifying the signal flow graph of Fig. 5 as follows. We simply move the directed edge from the source node to node 1 so that it is now directed from the source node to node 5 and is assigned a weight equal to $-J/J_*$, instead of unity (see Ref. 9 for a matrix formulation). The node $i$ ($i = 1, 2, 3, 4, 5$) in the resulting signal flow graph represents the flux-ratio control coefficient $C_i^R$. An expression for $C_i^R$ can be obtained in the usual manner by examining the directed paths from the source node to node $i$ and the corresponding nontouching cycles, if any, in the signal flow graph.

An alternate approach for assessing the regulatory effect of an enzyme on a branch-point flux is to define the flux control coefficients in Eqn. 19 with reference to that flux. For instance, to study the regulatory effects of the enzymes on the flux through the enzyme $E_5$, the flux control coefficients should be defined by Eqn. 19 with $J$ replaced by $J_5$. Under these circumstances, a different relationship exists among the flux control coefficients at the branch point (see, for example, Ref. 16). In keeping with this new branch-point relation, a procedure for drawing a signal flow graph analogous to that of Fig. 5 can be developed for the evaluation of the flux control coefficients. We shall not pursue this aspect further.

Additional complexities in pathway structure can be easily accommodated into a signal flow graph. Consider, as an example, the situation examined in Ref. 9 where the metabolite $X_4$ inhibits the second enzyme in pathway F. To account for this feedback loop, we treat the enzymes $E_2$ and $E_4$ as contiguous enzymes with $X_4$ as the adjoining metabolite (see Ref. 4). Accordingly, a directed edge of weight $\bar{\varepsilon}_4^2/\varepsilon_4^4$ should be included in Fig. 5 from node 2 to node 4, leading to the signal flow graph of Fig. 14. We have written $\varepsilon_4^2 = -\bar{\varepsilon}_4^2$, $\bar{\varepsilon}_4^2$ being the magnitude of the elasticity coefficient, $\varepsilon_4^2$, due to feedback inhibition. In this figure there are three first-order cycles in addition to those given in Fig. 6, and one second-order cycle in addition to those presented in Fig. 7. These additional cycles are shown in Fig. 15, which contribute to four more terms in the expression for $\Delta^\dagger$, in Eqn. 20. The flux control coefficient of enzyme $E_i$ in this pathway is found by examining the directed paths from the source node to node $i$, and all the nontouching loops with respect to each of these directed paths in Fig. 14. For the sake of brevity, further details are not given here. Alternatively, using the node elimination process described earlier, the signal flow graph of Fig. 14 may be appropriately simplified before evaluating the flux control coefficients

As a final note, we would like to mention that the method of signal flow graphs can also be used for control analysis of more complex pathways, such as those containing isozymes, substrate cycles and moiety-conserved cycles. A graph-theoretic treatment of these pathways will be presented in a future publication.

## Appendix A

Using the summation and connectivity theorems and branch point relationships, several authors have derived the governing equations for the control coefficients of a branched pathway, in terms of the enzyme elasticities and branch-point fluxes [7–9]. For pathway F, the equations for the flux control coefficients, when

Fig. 13. Conversion of node 1 into a source node in the signal flow graph of Fig. 5.

Fig. 14. A signal flow graph for the branched pathway F in which the enzyme $E_2$ is inhibited by the metabolite $X_4$.

Fig. 15. Parts (i)–(iii): three first-order cycles in Fig. 14, in addition to those shown in Fig. 6; part (iv): the second-order cycle in Fig. 14, in addition to those given in Fig. 7.

Fig. 16. An alternate signal flow graph of the branched pathway F.

Fig. 17. A signal flow graph for the branched pathway considered in Appendix C.

referred to the flux $J$, can be expressed in the matrix form $\mathbf{M} \cdot \mathbf{C} = \mathbf{b}$ as follows (see, for example Ref. 9).

$$\begin{pmatrix} 1 & 1 & 1 & 1 & 1 \\ -\bar{\varepsilon}_2^1 & \varepsilon_2^2 & 0 & 0 & 0 \\ 0 & -\bar{\varepsilon}_3^2 & \varepsilon_3^3 & 0 & \varepsilon_3^5 \\ 0 & 0 & -\bar{\varepsilon}_4^3 & \varepsilon_4^4 & 0 \\ 0 & 0 & -J_5 & -J_5 & J_* \end{pmatrix} \cdot \begin{pmatrix} C_1^J \\ C_2^J \\ C_3^J \\ C_4^J \\ C_5^J \end{pmatrix} = \begin{pmatrix} 1 \\ 0 \\ 0 \\ 0 \\ 0 \end{pmatrix}. \quad \text{(A-1)}$$

The first equation in Eqn A-1 is a statement of the summation theorem, and the last equation there is a consequence of the branch-point relationship; the remaining equations follow from the connectivity theorems of the various enzymes.

Eqn. A-1 is now written as follows. Divide each nonzero element on the $i$-th row of the matrix $\mathbf{M}$ by $-M_{ii}$, where $M_{ii}$ is the diagonal element on the $i$-th row. The resulting matrix equation is given by

$$\begin{array}{c} \begin{matrix} C_1^J & C_2^J & C_3^J & C_4^J & C_5^J \end{matrix} \\ \begin{pmatrix} -1 & -1 & -1 & -1 & -1 \\ \bar{\varepsilon}_2^1/\varepsilon_2^2 & -1 & 0 & 0 & 0 \\ 0 & \bar{\varepsilon}_3^2/\varepsilon_3^3 & -1 & 0 & -\varepsilon_3^5/\varepsilon_3^3 \\ 0 & 0 & \bar{\varepsilon}_4^3/\varepsilon_4^4 & -1 & 0 \\ 0 & 0 & J_5/J_* & J_5/J_* & -1 \end{pmatrix} \end{array} \cdot \begin{pmatrix} C_1^J \\ C_2^J \\ C_3^J \\ C_4^J \\ C_5^J \end{pmatrix} + \begin{pmatrix} 1 \\ 0 \\ 0 \\ 0 \\ 0 \end{pmatrix}$$

$$= \begin{pmatrix} 0 \\ 0 \\ 0 \\ 0 \\ 0 \end{pmatrix}. \quad \text{(A-2)}$$

where, for convenience, we have also written the unknown flux control coefficients horizontally above the 'coefficient' matrix. We will refer to them as flux control coefficients of the row vector, whereas the vector $C$ of the flux control coefficients will be referred to as the column vector.

From this matrix equation, the signal flow graph of Fig. 5 can be constructed in the following manner. First the nodes 1 through 5 are drawn designating the unknown flux control coefficients $C_i^J$ ($i = 1, 2, 3, 4, 5$). Next an edge is directed from each node representing the flux control coefficients in the row vector to each node representing the flux control coefficients in the column vector with the exception that if the flux control coefficients in the row vector is the same as that in the column vector, no edge is drawn; in other words, self-loops are not allowed. Each of these directed edges is assigned a weight equal to the corresponding matrix element. For example, the $-1$ element in (1,2) position is represented by a directed edge from node 2 to node 1 in the signal flow graph. Similarly, the element $J_5/J_*$ in (5,3) position is designated by an edge from node 3 to node 5, and so on. Of course, the zeros in this matrix do not lead to any edges in the signal flow graph. Finally a source node (i.e., node 6) is introduced and an edge of unity is directed from it to node 1, corresponding to the only nonzero element in the rightmost vector on the left hand side of Eqn. A-2.

## Appendix B

We present below an alternate procedure of constructing a signal flow graph for the control structure of the branched pathway F. First we treat the segment of this pathway containing the enzymes $E_1$, $E_2$ and $E_5$ as a linear pathway and draw its signal flow graph (without a source node); it consists of the nodes 1, 2 and 5 and their interconnecting edges (see Fig. 16). Next we treat the upper branch containing the enzymes $E_3$ and $E_4$ and the metabolite $X_4$ as part of a linear pathway and draw the corresponding signal flow graph (again, without a source node); it consists of the nodes 3 and 4 and the directed edges (3,4) and (4,3) in Fig. 16. Then, in keeping with the summation theorem for the entire pathway, an edge is drawn from each of the nodes 3 and 4 to node 1. The effect of branching in the original pathway is incorporated into the signal flow graph as follows. For the pair of enzymes $E_3$ and $E_5$ at the branch point, an edge is drawn from node 3 to node 5, carrying the weight $-\varepsilon_3^3/\varepsilon_3^5$; the ratio of the fluxes in the two branches are designated by a directed edge from node 5 to node 3 in Fig. 16. Finally, a source node (i.e., node 6) is introduced which is connected to node 1 by a directed edge of weight unity. It can be readily seen that Fig. 16 and Fig. 5 generate equivalent expressions for the flux control coefficients of the enzymes in pathway F.

## Appendix C

In this appendix we describe a systematic procedure for constructing a signal flow graph for a branched pathway containing any number of enzymes in each of its segments. Based on the results obtained from the signal flow graphs, we present a heuristic method for calculating the flux control coefficients of the enzymes directly from an inspection of the reaction pattern of the pathway (without drawing a signal flow graph). Consider, as an example, the following branched pathway containing two enzymes, $E_2$ and $E_3$, in its upper branch and three enzymes, $E_4$, $E_5$ and $E_6$, in its lower branch; the enzyme $E_1$ is in the segment containing the initial substrate $X_1$. The fluxes transmitted through the different segments are shown inside parentheses (Scheme G). We shall refer to the very first enzyme in the pathway (i.e., enzyme $E_1$) as the *leader* enzyme and the enzymes $E_2$ and $E_4$ as the *branch-point* enzymes.

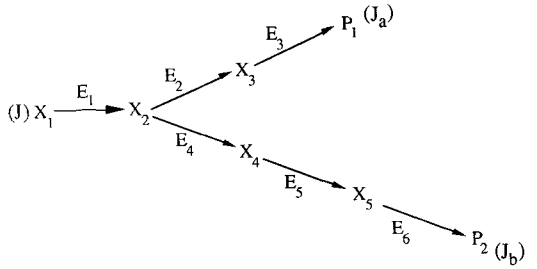


Scheme G

A signal flow graph characterizing the control structure of this pathway can be constructed by carrying out the following steps.

*Step 1.* Consider the initial-substrate containing segment and any one of the two dividing branches (say, the upper branch) as a linear pathway and draw its signal flow graph (without a source node). This signal flow graph consists of the nodes 1, 2 and 3 and their interconnecting edges (see Fig. 17). Identify the leader enzyme node (i.e., node 1) and the branch-point enzyme node (i.e., node 2).

*Step 2.* If the other dividing branch (i.e., the lower branch) contains more than one enzyme (which is the situation here), then treat all the enzymes (i.e., $E_4$, $E_5$ and $E_6$) and their adjoining metabolites as part of a linear pathway and draw the corresponding signal flow graph (again, without a source node). This signal flow graph consists of the nodes 4, 5 and 6 and their interconnecting edges (see Fig. 17). Identify the branch-point enzyme node (i.e., node 4) in this part of the signal flow graph.

*Step 3.* From each of the nodes in Step 2 (i.e., nodes 4, 5 and 6) draw a directed edge of weight $-1$ to the leader node (i.e., node 1), in keeping with the summation theorem for the entire pathway.

*Step 4.* From the branch-point enzyme node in Step 2 (i.e., node 4) direct an edge to the branch-point enzyme node in Step 1 (i.e., node 2), carrying a weight which is negative of the ratio of the elasticity coefficient of the branch-point enzyme in Step 2 (i.e., enzyme $E_4$) to that of the branch-point enzyme in Step 1 (i.e., enzyme $E_2$), with respect to the branch-point metabolite ($X_2$).

*Step 5.* From each of the nodes corresponding to the enzymes in the dividing branch in Step 1 (i.e., nodes 2 and 3), an edge is directed to the branch-point enzyme node in step 2 (i.e., node 4). Each of these edges is assigned to carry a weight which is equal to the ratio of the flux transmitted through the dividing branch in Step 2 to that through the dividing branch in Step 1.

*Step 6.* Introduce a source node (i.e., node 7) and connect it to the leader node by a directed edge of weight unity. This completes the construction of the signal flow graph which is shown in Fig. 17.

An alternate procedure of constructing a signal flow graph for this pathway is to treat the initial-substrate containing segment and the lower branch as a linear pathway (in Step 1) and carry out the remaining steps accordingly. This results in Fig. 18. The flux control coefficients of the various enzymes can be determined by examining the topology of Fig. 17 or Fig 18 in the manner discussed in the text. It is apparent that the above methodology can be used for a branched pathway containing an arbitrary number of enzymes in each of its segments.

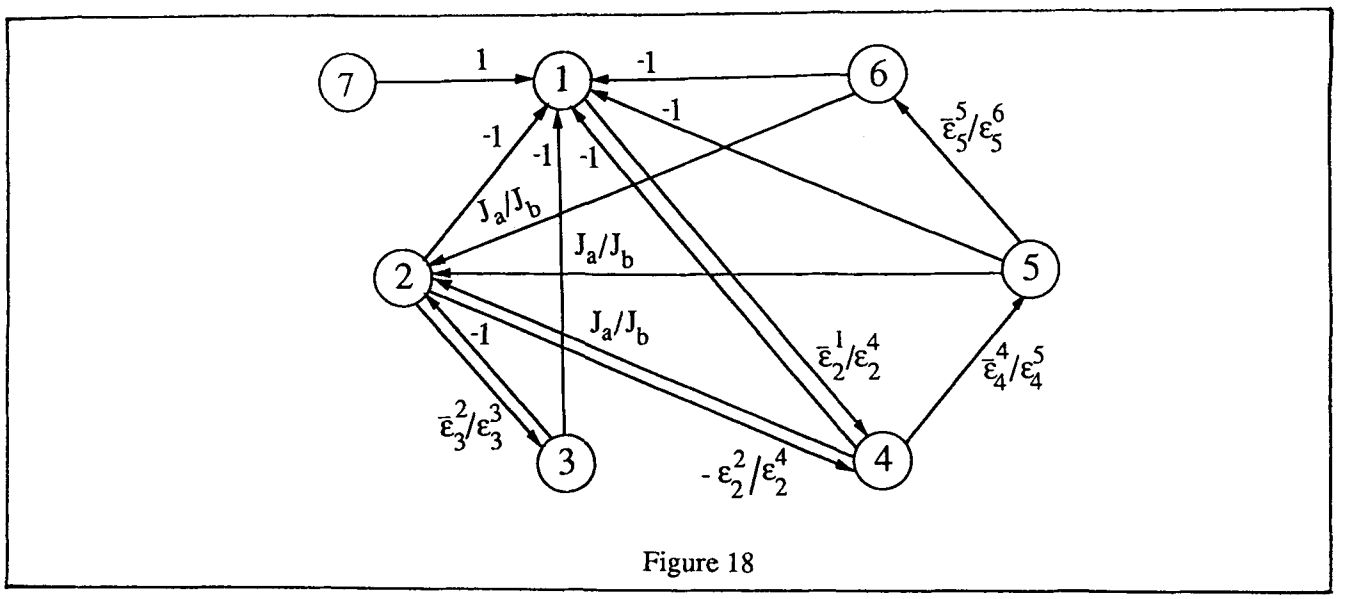


Figure 18

Fig. 18. An alternate signal flow graph for the branched pathway considered in Appendix C.

We now present a heuristic method for calculating the flux control coefficients of the enzymes directly from an inspection of the reaction sequence in the metabolic pathway (without drawing a signal flow graph). This method is based on the results obtained from the signal flow graph of Fig. 17 which was drawn by treating the initial-substrate containing segment and the upper branch as a linear pathway.

The flux control coefficient of an enzyme $E_i$ ($i = 1, 2, \ldots, 6$) in the pathway under consideration can be written in the form

$$C_i^J = N_i / \sum_{k=1}^{6} N_k.$$

The expressions for $N_i$ are obtained in the following manner. First of all, we ascertain the number of terms in $N_i$. If the enzyme $E_i$ lies in the initial-substrate containing segment of the pathway, then the number of terms in $N_i$ is equal to the total number of enzymes in the two dividing branches. On the other hand, if the enzyme $E_i$ lies on one of the dividing branches, then the number of terms in $N_i$ equals the number of enzymes present in the other dividing branch.

In order to evaluate $N_i$, we now consider the upper and lower branches separately and form the following expressions consisting of the continued products of the ratios of the magnitudes of the elasticity coefficients of contiguous pairs of enzymes in each branch and unity:

$$H_a = 1 + \frac{\bar{\varepsilon}_3^2}{\varepsilon_3^3}, \text{ and } H_b = 1 + \frac{\bar{\varepsilon}_4^4}{\varepsilon_4^5} + \frac{\bar{\varepsilon}_4^4 \bar{\varepsilon}_5^5}{\varepsilon_4^5 \varepsilon_5^6},$$

for the upper and lower branches, respectively. We also form the product of the ratios of the magnitudes of the elasticity coefficients of *all* contiguous pairs of enzymes in the initial-substrate containing segment and the branch-point enzyme $E_2$ located on the upper branch; since there is only one enzyme in the initial-substrate containing segment of the pathway under consideration, this is simply equal to $\bar{\varepsilon}_2^1/\varepsilon_2^2$; we will call this product $S_{22}$, referring to the branch-point enzyme $E_2$ and the metabolite $X_2$. Let us first evaluate $N_2$ for the flux control coefficient of the enzyme $E_2$, which is the branch-point (i.e., the first) enzyme in the upper branch. This is obtained by multiplying $H_b$ and $S_{22}$. It follows that

$$N_2 = \frac{\bar{\varepsilon}_2^1}{\varepsilon_2^2} H_b = \frac{\bar{\varepsilon}_2^1}{\varepsilon_2^2}\left(1 + \frac{\bar{\varepsilon}_4^4}{\varepsilon_4^5} + \frac{\bar{\varepsilon}_4^4 \bar{\varepsilon}_5^5}{\varepsilon_4^5 \varepsilon_5^6}\right).$$

The $N_i$ for the flux control coefficient of any other enzyme $E_i$ in the upper branch is derived by multiplying $N_2$ with the continued product of the ratios of the magnitudes of the elasticity coefficients of the enzymes $E_2$ through $E_i$ in that branch. For instance, $N_3$ is given by

$$N_3 = \frac{\bar{\varepsilon}_2^1 \bar{\varepsilon}_3^2}{\varepsilon_2^2 \varepsilon_3^3} H_b = \frac{\bar{\varepsilon}_2^1 \bar{\varepsilon}_3^2}{\varepsilon_2^2 \varepsilon_3^3}\left(1 + \frac{\bar{\varepsilon}_4^4}{\varepsilon_4^5} + \frac{\bar{\varepsilon}_4^4 \bar{\varepsilon}_5^5}{\varepsilon_4^5 \varepsilon_5^6}\right).$$

The $N_i$'s for the flux control coefficients of the enzymes in the lower branch are written down as follows. For the first enzyme $E_4$, which is the branch-point enzyme in this branch, we write

$$N_4 = \frac{\bar{\varepsilon}_2^1}{\varepsilon_2^2} \frac{J_b}{J_a} H_a = \frac{\bar{\varepsilon}_2^1}{\varepsilon_2^2}\left(1 + \frac{\bar{\varepsilon}_3^2}{\varepsilon_3^3}\right) \frac{J_b}{J_a},$$

which is obtained by forming the product of $S_{22}$, $H_a$ and the ratio $(J_b/J_a)$ of the fluxes in the lower and upper branches. An expression for $N_5$ is derived by multiplying $N_4$ with the ratio of the magnitudes of the elasticity coefficients of the enzymes $E_4$ and $E_5$, with respect to $X_4$:

$$N_5 = \frac{\bar{\varepsilon}_2^1 \bar{\varepsilon}_4^4}{\varepsilon_2^2 \varepsilon_4^5} \frac{J_b}{J_a} H_a = \frac{\bar{\varepsilon}_2^1 \bar{\varepsilon}_4^4}{\varepsilon_2^2 \varepsilon_4^5}\left(1 + \frac{\bar{\varepsilon}_3^2}{\varepsilon_3^3}\right) \frac{J_b}{J_a}.$$

Similarly, using the continued product of the ratios of the magnitudes of the elasticity coefficients of the enzymes $E_4$, $E_5$ and $E_6$, we have

$$N_6 = \frac{\bar{\varepsilon}_2^1 \bar{\varepsilon}_4^4 \bar{\varepsilon}_5^5}{\varepsilon_2^2 \varepsilon_4^5 \varepsilon_5^6} \frac{J_b}{J_a} H_a = \frac{\bar{\varepsilon}_2^1 \bar{\varepsilon}_4^4 \bar{\varepsilon}_5^5}{\varepsilon_2^2 \varepsilon_4^5 \varepsilon_5^6}\left(1 + \frac{\bar{\varepsilon}_3^2}{\varepsilon_3^3}\right) \frac{J_b}{J_a}.$$

Finally, for the flux control coefficient of the very first enzyme in the initial-substrate containing segment, we may write

$$N_1 = H_b + \frac{\varepsilon_2^4}{\varepsilon_2^2} \frac{J_b}{J_a} H_a.$$

The second term on the right hand side of this equation is formed by the product of the ratio of the elasticity coefficients of the branch-point enzymes, $E_4$ and $E_2$ with respect to $X_2$, the ratio of the fluxes, $J_b/J_a$, in the lower and upper branches, and $H_a$. If follows that

$$N_1 = 1 + \frac{\bar{\varepsilon}_4^4}{\varepsilon_4^5} + \frac{\bar{\varepsilon}_4^4 \bar{\varepsilon}_5^5}{\varepsilon_4^5 \varepsilon_5^6} + \frac{\varepsilon_2^4}{\varepsilon_2^2}\left(1 + \frac{\bar{\varepsilon}_3^2}{\varepsilon_3^3}\right) \frac{J_b}{J_a}.$$

If the initial-substrate containing segment contains more enzymes (between the enzyme $E_1$ and the metabolite $X_2$), then the $N_i$ for each of these intermediary enzymes can be expressed as $N_1$ times the continued product of the ratios of the magnitudes of the elasticity coefficients of the enzymes $E_1$ up to that specific enzyme.

An analogous procedure can be devised for deriving the expressions for $N_i$, consistent with the signal flow graph of Fig. 18, which was drawn by treating the initial-substrate containing segment and the lower branch as a linear pathway. We may write

$$N_2 = \frac{\bar{\varepsilon}_2^1}{\varepsilon_2^4}\frac{J_a}{J_b}H_b, \quad N_3 = \frac{\bar{\varepsilon}_2^1\bar{\varepsilon}_3^2}{\varepsilon_2^4\varepsilon_3^3}\frac{J_a}{J_b}H_b,$$

$$N_4 = \frac{\bar{\varepsilon}_2^1}{\varepsilon_2^4}H_a, \quad N_5 = \frac{\bar{\varepsilon}_2^1\bar{\varepsilon}_4^4}{\varepsilon_2^4\varepsilon_4^5}H_a, \quad N_6 = \frac{\bar{\varepsilon}_2^1\bar{\varepsilon}_4^4\bar{\varepsilon}_5^5}{\varepsilon_2^4\varepsilon_4^5\varepsilon_5^6}H_a,$$

and

$$N_1 = H_a + \frac{\varepsilon_2^2}{\varepsilon_2^4}\frac{J_a}{J_b}H_b.$$

In writing down the expressions for the $N_i$'s by the above procedures we have adopted the following convention regarding the appearance of the flux ratio in relation to the elasticity coefficients $\varepsilon_2^2$ or $\varepsilon_2^4$ of the branch-point enzymes $E_2$ or $E_4$. If the enzyme $E_i$ for which we want to write down an expression of $N_i$ lies, say, on the upper branch and the elasticity coefficient $\varepsilon_2^2$ (of the branch-point enzyme $E_2$ lying on the same branch) is used in $N_i$ through $S_{22}$, then $N_i$ will not contain the flux ratio of the two branches. If, on the other hand, the elasticity coefficient $\varepsilon_2^4$ (of the branch-point enzyme $E_4$ lying on the other, i.e., lower branch) is used in writing down $N_i$, then $N_i$ will contain the ratio of fluxes transmitted through the two branches. See, for example, the expressions for $N_2$ or $N_3$ written according to the two procedures described above. A similar strategy is used in writing down the expression for $N_i$ of an enzyme located on the lower branch; see the expressions for $N_4$, $N_5$ or $N_6$. The symmetry in the expressions for $N_1$ written by the two procedures is apparent. It is a simple exercise to show that both procedures yield equivalent expressions for the flux control coefficients of the various enzymes.

Finally, we would like to mention that the heuristic methods described above can also be devised by solving the governing equations (namely, the summation theorem, connectivity theorems and branch-point relation) for the flux control coefficients by means of algebraic techniques such as matrix inversion or Gaussian elimination, and selectively grouping the terms in the expression for each control coefficient.

## References


1 Mason, C.J. (1953) Proc. IRE 41, 1144–156.
2 Chen, W.K. (1971) Applied Graph Theory, North-Holland Series in Applied Mathematics and Mechanics, Vol. 13, Amsterdam, The Netherlands.
3 Chua, L.O. and Lin, P.M. (1975) Computer-Aided Analysis of Electronic Circuits: Algorithms and Computational Techniques, Prentice Hall, New Jersey.
4 Sen, A.K. (1990) Biochem. J. 269, 141–147.
5 Kacser, H. and Burns, J.A. (1973) Symp. Soc. Exp. Biol. 27, 65–104.
6 Heinrich, R. and Rapoport, T. (1974) Eur. J. Biochem. 42, 89–102.
7 Fell, D.A. and Sauro, H.M. (1985) Eur. J. Biochem. 148, 555–561.
8 Small, J.R. and Fell, D.A. (1988) J. Theor. Biol. 136, 181–197.
9 Westerhoff, H.V. and Kell, D.B. (1987) Biotech. Bioeng. 30, 101–107.
10 Hofmeyr, J.H.S. (1989) Eur. J. Biochem. 186, 343–354.
11 Sen, A.K. (1990) Biochem. J. 272, 65–70.
12 Sen, A.K. (1990) Int. J. Biochem. 22, 1295–1301.
13 Sen. A.K. (1990) Math. Biosci. 102, 191–223.
14 Sen. A.K. (1990) Biochem. J. 275, 253–258.
15 Reder, C. (1988) J. Theor. Biol. 135, 175–201.
16 Barrett, J. (1989) Biochim. Biophys. Acta 992, 369–374.